Hindawi Publishing Corporation
Journal of Nanomaterials
Volume 2012, Article ID 486301, 21 pages
doi:10.1155/2012/486301

Review Article

Nanostructures for Medical Diagnostics

Md. Motasim Bellah,[1,2] Shawn M. Christensen,[3] and Samir M. Iqbal[1,2,4,5]

[1] *Department of Electrical Engineering, University of Texas at Arlington, Arlington, TX 76011, USA*
[2] *Nanotechnology Research and Teaching Facility, University of Texas at Arlington, Arlington, TX 76019, USA*
[3] *Department of Biology, University of Texas at Arlington, Arlington, TX 76010, USA*
[4] *Joint Graduate Committee of Bioengineering Program, University of Texas at Arlington, Arlington, TX 76010, USA*
[5] *Department of Bioengineering, University of Texas at Arlington, Arlington, TX 76010, USA*

Correspondence should be addressed to Samir M. Iqbal, smiqbal@uta.edu

Received 22 June 2011; Revised 30 September 2011; Accepted 19 October 2011

Academic Editor: Xing J. Liang

Nanotechnology is the art of manipulating materials on atomic or molecular scales especially to build nanoscale structures and devices. The field is expanding quickly, and a lot of work is ongoing in the design, characterization, synthesis, and application of materials, structures, devices, and systems by controlling shape and size at nanometer scale. In the last few years, much work has been focused on the use of nanostructures toward problems of biology and medicine. In this paper, we focus on the application of various nanostructures and nanodevices in clinical diagnostics and detection of important biological molecules. The discussion starts by introducing some basic techniques of micro-/nanoscale fabrication that have enabled reproducible production of nanostructures. The prospects, benefits, and limitations of using these novel techniques in the fields of biodetection and medical diagnostics are then discussed. Finally, the challenges of mass production and acceptance of nanotechnology by the medical community are considered.

1. Introduction

By definition, a nanostructure is an object that has at least one dimension equal to or smaller than 100 nanometers. There is a wide variety of nanostructures, such as nanoparticles, nanopores, nanorods, nanowires, nanoribbons, nanotubes, and nanoscaffolds. The most promising features of these structures are their size-dependent properties. For example, metallic nanoparticles exhibit tunable radiation and absorption wavelength depending on their aspect ratio [1] and coating [2]. These unique properties are attributed to the phenomenon called localized surface plasmon resonance (LPSR). Each particle can effectively produce photoluminescence equivalent to a million dye molecules. Additionally, they are photostable and do not suffer from photobleaching [3]. Owing to their superior optical properties, they can produce better signal over ordinary dye molecules. After coating with probe molecules, the optical properties of nanostructures allow the detection of specific target molecules.

Some nanostructured surfaces are known to be suitable for enhanced cell adhesion and proliferation [4, 5]. This is believed to stem from mimicking the actual nanofeatures of the living systems [6]. Carbon nanotubes exhibit exceptionally high current carrying capacity [7, 8]. They can be used to interconnect devices at very low dimensions where ordinary metals suffer from high contact resistance and electromigration. Electromigration limits the use of the most widely used interconnect metal, copper, at nano-scale. Nanowires are reported to be useful in different sensing techniques including electrical, electrochemical, optical, and mass-based approaches [9–12]. Usually nanowires show high resistance due to the surface scattering of carriers, but their resistance is strongly dependent on the species attached on the surface. If the immobilized species can selectively bind to a target, then it can detect an ultralow concentration of target species [13–15].

Early detection is very crucial for some diseases like cancer to provide better treatment. Early detection increases the probability of curing diseases and significantly improves

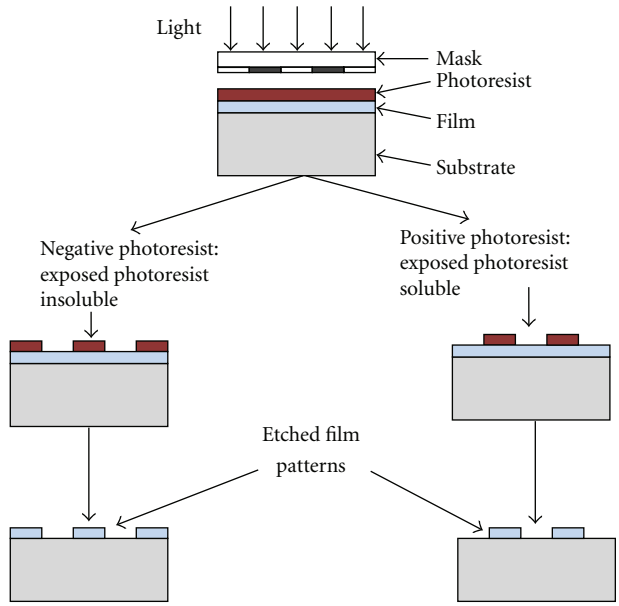

Figure 1: Photolithography using negative or positive photoresist.

the rate of mortality. Historically, it has been difficult to detect early or precancerous states due to unavailability of ultra-sensitive devices capable of detecting a multivariate disease like cancer. But now, such devices may be realizable using a large number of nanostructures on a single assay system [16, 17].

There are two different approaches for fabricating nanostructures irrespective of the field of applications: top down and bottom up.

In top-down approach, a bulk material is laterally patterned by a series of subtractive and additive steps. The basic fabrication steps in a top-down approach are (i) lithography, (ii) oxidation, (iii) etching, (iv) ion implantation, (v) diffusion, and (vi) deposition.

(i) Lithography: lithography is the process of transferring a pattern from a mask on to a substrate. Optical lithography, generally called photolithography, has been the workhorse of semiconductor industry. Newer techniques, called next-generation lithography (e.g., e-beam/ion-beam lithography, X-ray lithography, nanoimprint lithography, scanning probe lithography, interference lithography, nanotemplating, etc.) are more of experimental nature but are expected to replace photolithography. Photolithography requires a mask that contains the template features on it. A photosensitive material (photoresist) is spun cast on the substrates which undergoes changes in chemical composition when exposed optically to a specific wavelength of light through the mask. The exposed wafer is then developed in a solution (developer solution such as MF-319) to create the pattern. A typical photolithography process is shown in Figure 1 (adapted from [18]).

(ii) Oxidation: it is the formation of silicon dioxide (SiO_2) on a silicon substrate [18]. There are several techniques for growing SiO_2 on a silicon substrate; more common are thermal oxidation, plasma anodization, and wet anodization. Among these, thermal oxidation is used in large-scale integration of electronic devices. A silicon wafer is placed in a furnace and exposed to high temperature either with or without water vapor. There are thus two types of thermal oxides: oxides made via dry oxidation and oxides made via wet oxidation. In dry oxidation, a mixture of nitrogen and oxygen is pumped into the furnace (which is already at or above 1000°C). At high temperature, silicon reacts with oxygen and a SiO_2 layer is grown. In wet oxidation, water vapor instead of oxygen is pumped into the chamber along with nitrogen. The growth rates of oxide in both cases depend on the temperature, pressure, orientation of the wafer, dopant species in the wafer, moisture content inside the chamber, presence of chlorine, and so forth. Thermally grown oxides are used as tunneling oxide, gate oxide in metal oxide field effect transistors (MOSFETs), dielectric material in capacitors, masking material against ion implantation and diffusion, passivation layer on the substrate, device isolating material, and so forth [18].

(iii) Etching: etching is a subtractive method that selectively removes material from the substrate. A mask pattern is first created on the layer to be etched. Then the etchant is introduced into the system. This can be done in dry or wet conditions, depending on the requirements. Wet etching offers a high etching rate, but it is mostly isotropic, which is sometimes not desired. On the other hand, dry etching is highly directional in nature but less selective compared to wet etching. Dry etching is preferred over wet etching where a high aspect ratio needs to be achieved. Almost every lithography step is followed by an etching step to create patterns.

(iv) Ion Implantation: ion implantation is a process in which energetic, charged atoms (or molecules) are directly introduced into the substrate. It is the process of introducing impurities in a controlled fashion. The distribution of the impurity atoms depend on the type of particles, their energy, and the orientation of the wafer with respect to the ion beam.

(v) Diffusion: diffusion is the spontaneous movement of particles toward a lower concentration region due to the concentration gradient. It is used to introduce dopants in crystal. It is a high temperature process.

(vi) Deposition: this process is used for putting uniform layers of materials onto substrates. It can be chemical vapor deposition (CVD) or physical vapor deposition (PVD), as depicted in Figure 2 [18]. In CVD the reactant species are introduced into the chamber. These react with each other and deposit a layer of one product material. The rest of the byproducts are usually gaseous and are pumped out of the chamber. CVD offers uniform, robust, and high throughput deposition of materials. It can be used to deposit a wide variety of materials, including Si_3N_4, SiO_2, Al, and W. PVD is a physical process where a target material may be vaporized using heat or an electron beam. The evaporated atoms or molecules are deposited on the surface of the substrate. No chemical reaction occurs in this process. Since there is no other material inside the chamber, PVD offers purer deposited films than CVD, but the throughput is lower for a PVD system [18].

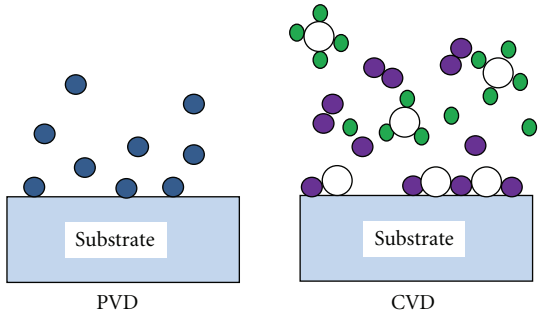

Figure 2: Chemical vapor deposition (CVD) and physical vapor deposition (PVD), adapted from [18].

The top-down approach can be used to fabricate a wide variety of devices with high reliability and high integrity; thus, this approach is common in the semiconductor device industry. Many of the novel nanostructures, like nanowires and nanopores, may be fabricated with top-down approaches [19–23]. Stern et al. reported nanowires fabricated by the top-down approach that were used to detect biological samples without any labeling [21]. Nanopores can be used to detect and measure biophysical properties of DNA, proteins and many other molecules passing through the nanopores [22, 24, 25].

The major advantages of the top-down approach are that a large number of features can be transferred onto a substrate from a mask by a single exposure and that single mask can be used many times. Successive masks can be aligned with high precision using alignment marks placed on the substrate. Owing to the parallel nature of the top-down approach, high density devices can be produced at mass-scale. In last few decades, advances in top-down fabrication has led to a monotonic decrease of device dimensions, thereby increasing the density of devices on a single chip. The immediate consequence has been significant reduction in cost per device.

However, at very small scales (less than 100 nm), the top-down approach has inherent limitations [26]. Optical lithography, which has been the key enabler of low cost mass production of micro-/nanodevices, is no longer suitable to fabricate structures below 100 nm. When the wavelength gets too small, conventional lenses cannot be used to focus light due to the high optical absorption [26]. New equipment would be required to focus the light, adding to production cost.

In bottom-up fabrication, the building blocks (e.g., the atoms or molecules) are brought in close proximity to form the desired structures. The assembling of the elementary blocks is usually manipulated by physical aggregation, chemical reaction, and use of templates [27]. Controlled chemical reactions are used to manipulate those blocks to self-assemble and make nanostructures such as nanotubes, nanoribbons, and quantum dots [28, 29]. There are two methods to achieve self-assembly: templating and nontemplating. Templating involves the interaction of biomacromolecules under the influence of a specific sequence, pattern, structure, external force, or spatial constraint. For instance, cylindrical amphiphilic polymeric micelles may be used as templates to fabricate semiconducting nanotubes of cadmium sulphide. Semiconducting cadmium sulphide may be used to detect a DNA sequence via field effect transistor (FET) action [30]. In contrast, nontemplating is the formation of larger structures by individual atoms or molecules without external influence [31, 32]. For example, nontemplating can be used to form a variety of structures and shapes, including twins, tetramers, rods, triangles, and 3D arrays [32]. Self-assembly is a cost-effective and efficient technique that can be used to produce nanostructures and features below 100 nm [33].

The bottom-up approach accommodates a wide range of possibilities in the design and fabrication of molecular devices. The unique advantage of the bottom-up approach is the potential to assemble nanostructures where the top-down approach fails. Even with sophisticated photolithography, it is not easy to fabricate nanostructures at a size of a few nanometers. Self-assembly is an ideal approach in this case [34]. Nonetheless, one of the major challenges of this approach is to ensure predefined structures with precise shapes and sizes. Hierarchical design, which makes the top-down approach suitable for producing high density devices, is not yet feasible with the bottom-up approach.

2. Medical Applications of Nanostructures

Nanodiagnostics is defined as the use of nanotechnology for clinical diagnostic purposes [35, 36]. Recently, a wide variety of nanostructures has been tested in different diagnostics applications. Nanostructure-based diagnostics have the promise to offer higher sensitivity and specificity, allowing earlier detection of diseases [36]. The increased demand for sensitivity requires the occurrence of a diagnostically significant interaction between analyte molecules and signal-generating parts, thus enabling detection of a very low amount of analyte. Due to their increased sensitivity and selectivity, different nanostructure-based assays have opened new directions in diagnostics of pathogens and diseases in the last few years [36]. The novel and unique characteristics of nanostructure-based diagnostics have the potential to create point-of-care applications. The applications of different nanostructures in the field of diagnostic and detection are reviewed below.

2.1. Nanostructured Surfaces. Nanoscale topography is achieved on a substrate by using a number of techniques. Nanostructured or more precisely nanotextured surfaces show interesting properties. For example, nanotextured surfaces have been shown to enhance adsorption of cells and increase cell proliferation [37, 38]; nanopillars on a polyethylene glycol (PEG) surface patterned by UV-mediated capillary lithography have been shown to enhance the adsorption of proteins [39]. The nanopatterned surface in the latter case also enhanced the cell adhesion (heart fibroblasts of natal rat). The enhanced adhesion was explained in terms of the increased surface area, and the resulting increase in interactions between the cells and the functional group on the surface [39]. Antibody

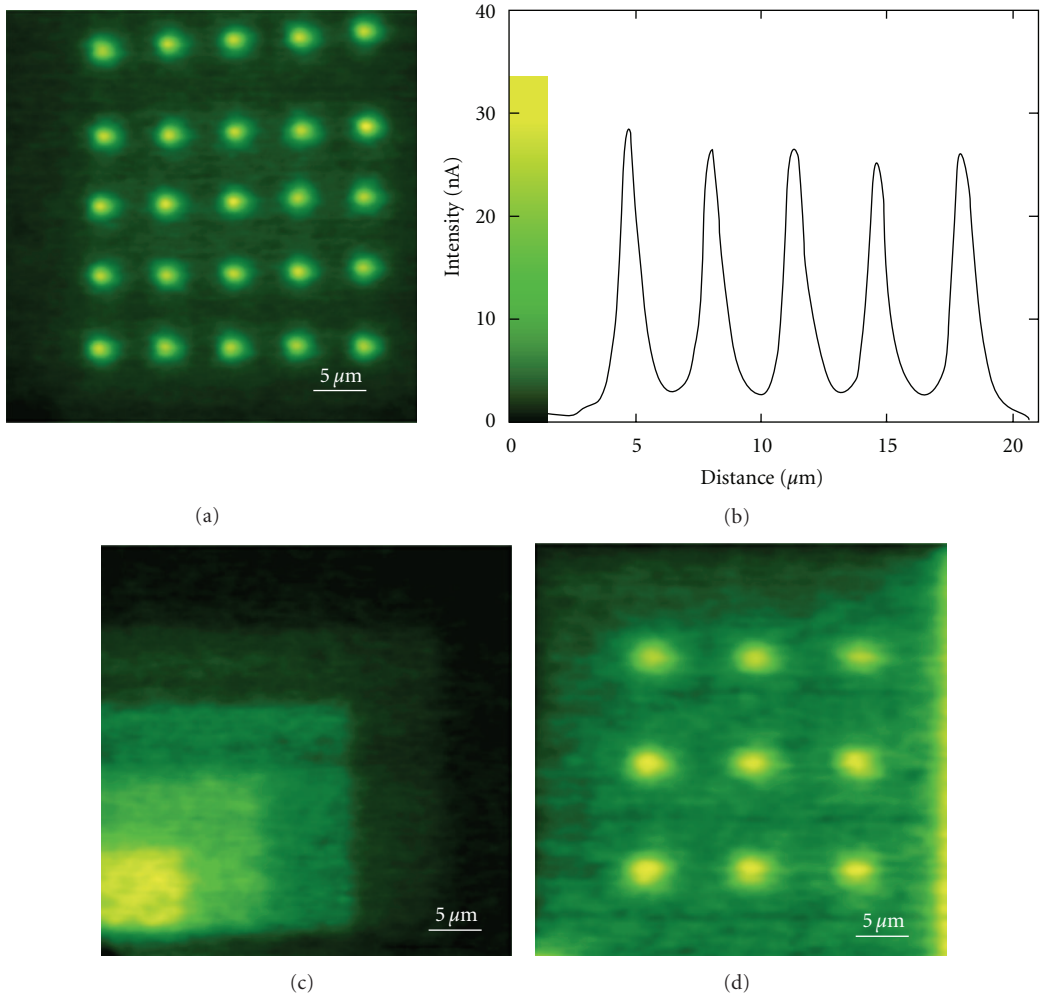

Figure 3: Fluorescence images of (a) biotinylated DNA deposited on to a streptavidin-coated glass surface; (b) intensity plot across the bottom row of (a); (c) pattern of biotinylated DNA square on top of another; (d) G-protein dots on a positively charged glass surface, reprinted with permission from [42]. Copyright 2002 American Chemical Society.

functionalized nanostructured surfaces have also been used to detect specific proteins or cells [40]. The increased adhesion has been shown to impart more sensitivity in the detection. Additionally, these structures are simple to fabricate and to reproduce. The structures are robust enough to remain stable upon exposure to solvents like water and ethanol [39].

Dip pen nanolithography (DPN) is a scanning probe lithography technique that can directly write patterns of molecules like modified oligonucleotides and mercaptopropyltrimethoxysilane (MPTMS) on silicon dioxide chips [41]. Fluorophore-labeled complementary and noncomplementary DNA molecules have been used to verify the specificity of the patterned molecules. The same array could be reused after rinsing with deionized (DI) water to assemble the modified complimentary DNA.

Andreas et al. reported a straightforward method to create patterns by direct writing of DNA and proteins on a glass surface by scanning ion conductance microscopy (SICM). Reportedly, their method possessed delivery control down to the single molecule level [42]. Fluorophore-labeled DNA and G protein were patterned on a glass surface, and images were taken as shown in Figure 3. These methods can be used to fabricate DNA and protein arrays [41, 42]. Antibodies and complementary DNA tagged with fluorophore or nanoparticles could be detected by these arrays. Though this nanopatterning technique is still at its nascent level, it shows the potential to possibly miniaturize certain medical diagnostic assays as this novel technique can utilize very small sample volumes to detect target molecules.

Recently, nanoarrays of monoclonal antibodies have been created by DPN to capture HIV p24 proteins from human plasma samples. AFM was used to determine the presence of p24 after capture. By adding anti-p24-modified gold nanoparticles which would selectively bind to the p24 spot, a detection limit of 0.025 pg/mL was achieved. This detection level is much better than the 5 pg/mL limit of conventional enzyme-linked immunosorbent assay (ELISA) [43].

A capacitor is an electrical device that is formed when an insulating material is sandwiched between two electrode

plates. When the gap between two plates is a few nanometers, it can be called a nanocapacitor. The capacitance can be determined from the plate area, the distance between plates, and the dielectric properties of the insulating medium. The working principle of a nanocapacitor-based biodetection device is simple: if some target molecule selectively could be attached onto a dielectric material, it would change the dielectric constant of the material appreciably, and the change in capacitance would be significant. This change could be measured electrically, allowing detection of the target molecules. The main advantage of this method is that it does not require any prior labeling of the sample. The only requirement is that there should be a minimum concentration of target molecules present in the sample sufficient to create appreciable change in capacitance. Kang et al. developed transparent nanocapacitors that were used to monitor dielectric and optical dynamic behavior of biomolecules. They used planar nanogap capacitors with 50 nm gaps, fabricated using silicon nanolithography [44]. The nanogap was created by in-plane sacrificial oxide etching. The single stranded DNA (ssDNA) was immobilized on the electrode surface. When the target DNA hybridized with the probe DNA, the dielectric property changed, resulting in a change in capacitance. The permittivity changed upon hybridization, which implied that the capacitance changed accordingly [44]. Permittivity was significantly increased in the case of hybridization, allowing detection of complimentary DNA. A large two-dimensional array of such nanocapacitors can be used for label-free measurement of nucleic acid targets with high sensitivity.

2.2. Nanoparticles. Nanoparticles are ultrafine particles with at least one of the diameters (major or minor axis) less than 100 nm [45]. There is a wide variety of nanoparticles depending on their shapes, materials, and sizes. The most common shapes of nanoparticles are sphere, rod, prism, dot, star, and so forth. Nanoparticles can be synthesized from metals or polymers [46, 47]. Among metallic nanoparticles, gold nanoparticles (GNPs) are used extensively for many applications and especially in bioassays [46]. There are several techniques to produce GNPs. Most commonly, GNPs are synthesized by chemical reduction of a precursor compound of gold in the presence of a capping agent (such as $AuClO_4$) [48]. This capping agent is able to bind to the GNP surface, blocking its growth beyond the nanometer range and stabilizing the colloid in a particular solvent. This method is commonly used to produce spherical GNPs [48]. Temperature, reducing agent, capping agent, and reaction time are the experimental parameters to control the shape and size of the GNPs [49].

Quantum dots (QDs) and GNPs can be used to develop immunoassays to detect pathogens and DNA sequence [50]. Used as fluorophores, these nanoparticles can produce six orders of magnitude stronger emission intensity than conventional dyes. Properties like high photostability, single-wavelength excitation and size-tunable emission make QDs and GNPs very suitable for imaging purposes [51]. GNPs have also been widely used in optical detection systems due to their very high absorption coefficients [52]. The optical properties of GNPs and QDs (such as absorption coefficient, refractive index, color, etc.) can be explained from a phenomenon called surface plasmon resonance (SPR). The emission bands of NPs and QDs strongly depend on their shapes rather than sizes and are not perturbed by refractive index of the surrounding medium [52].

GNPs can be detected by optical absorption, Raman scattering, fluorescence, magnetic/atomic force microscopy, and electrical resistance measurements. The availability of these various detection methods makes GNPs useful markers [53]. GNPs with attached DNA and Raman-active dyes have been shown to assemble on a sensor surface to detect the presence of complementary DNA target. Surfaces patterned with multiple DNA strands have the potential to detect different DNA sequences simultaneously [36].

Zhang et al. demonstrated a quantum dot-fluorescence-resonance-energy- transfer (QD-FRET) based nanosensor. In the presence of target DNA, the reporter probe and the capture probes were sandwiched as shown in Figure 4 [54]. The assembly was then attached to the QD with the help of a capture probe. When this complex was excited with a laser source, it emitted two characteristic wavelengths: one for the QD and one for the reporter molecule. In the absence of the target molecule, there was emission only from QD. However, if the target was present, then emissions from QD and reporter molecules both were detected [54].

For separation-free DNA hybridization detection, molecular beacons are the most widely used biomolecules. A background noise comparison between the QD-FRET-based nanosensor and the molecular beacon is presented in Figure 5. From Figure 5(a) it can be seen that the background fluorescent signal kept increasing with the increase of probe concentration, whereas the QD-FRET-based nanosensor showed almost zero noise irrespective of the probe concentration. Comparison of detection sensitivity, defined as the ratio of the fluorescent burst after and before introducing the targets is shown in Figure 5(b). At every level of target concentration, the nanosensor showed higher responsivity. The nanosensor showed almost 100-fold higher responsivity than the molecular beacon at a target concentration of 0.96 nM. Also, this QD-based sensor had the sensitivity as low as 4.8 fM, which is 10,000 times lower than that achieved by the molecular beacons [54]. The QD-based sensing technique shows promise in the detection of oligonucleotides, proteins and polypeptides. The main advantages of the platform are that it produces results in real time and at the single molecule level; therefore, it can be used to study molecular interactions with high temporal and spatial resolution [54].

An electrical resistance measurement system can also be used to detect the hybridization between the probe and target molecules. In one report, capture strands of DNA were attached in between electrode gap first, then the GNP-modified probing strands were dispensed on the surface [50]. A mixture of silver nitrate and hydroquinone was used to enhance the conductivity of the gap. When the target strands were present in the sample solution, they hybridized to the capture strands and GNP probes onto the surface, and the resistance kept reducing as the time went by [50]. It was

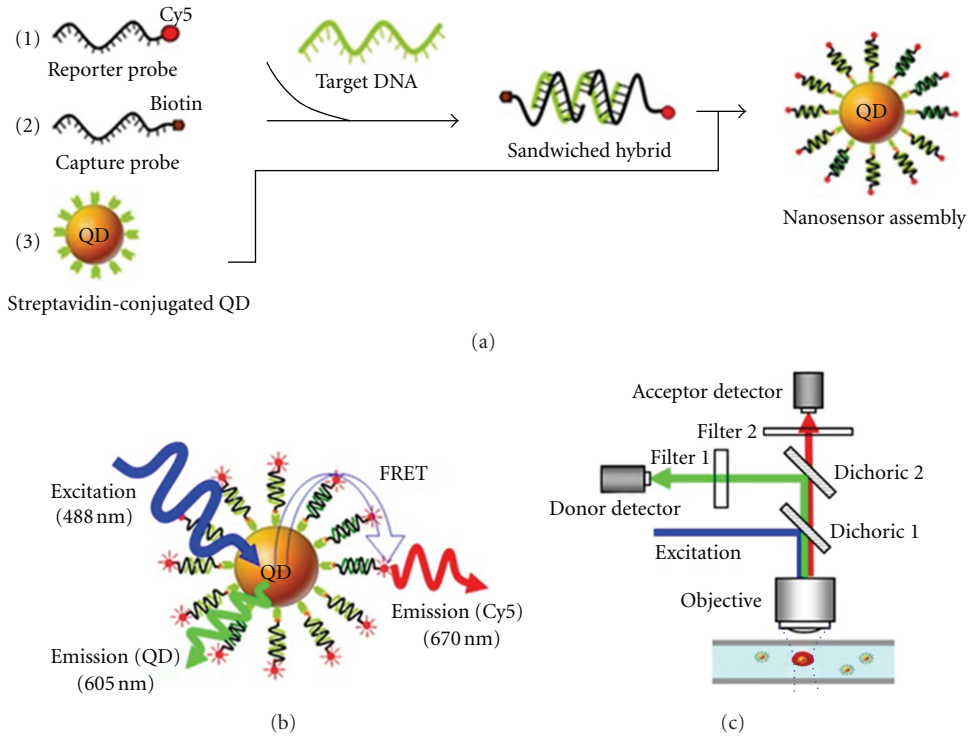

FIGURE 4: Schematic diagram of single-QD-based DNA nanosensors: (a) functionalized QD in the presence of target molecules; (b) mechanism of fluorescence emission from Cy5 upon illumination. It is caused by FRET between Cy5 acceptors and a QD donor; (c) experimental setup, reprinted by permission from Nature Publishing Group: Nature Materials [54], copyright 2005.

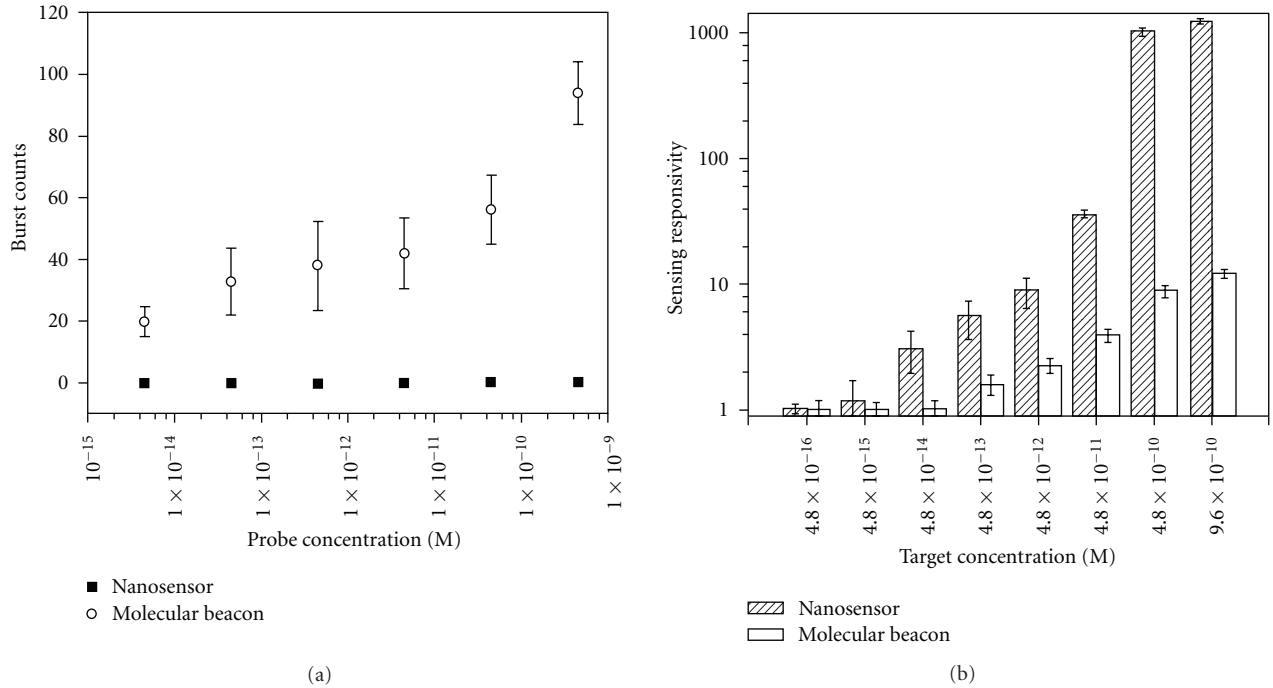

FIGURE 5: Performance of QD-based nanosensor. (a) Fluorescent burst counts versus probe concentration plot for QD-based nanosensors and molecular beacons. The concentration ratio of the Cy5-labelled reporter probe and the biotinylated capture probe was 1 : 1, and the Cy5/QD ratio was maintained at 24 in all experiments. The molecular beacons were Cy5-5-CGACC CCTGC CACGG TCTGA GA GGTCG-3-BHQ-2 (stems are underlined). Measurement time was 100 s. (b) Sensing responsivity versus target concentration plot for nanosensors and molecular beacons. Concentrations of receptor, capture probe, and molecular beacon were all 4.8×10^{-10} M and concentration of QD was 2×10^{-11} M, reprinted by permission from Nature Publishing Group: Nature Materials [54], copyright 2005.

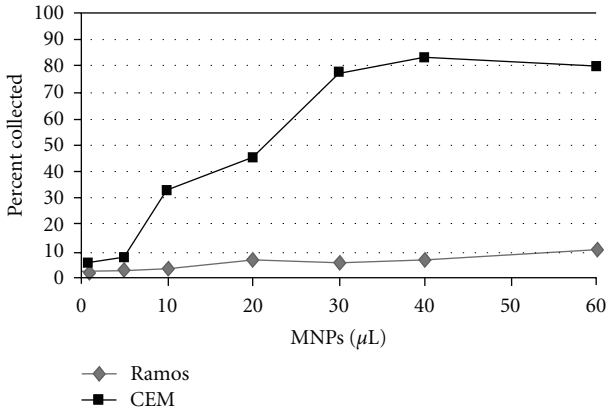

Figure 6: Extraction efficiency of magnetic nanoparticles (MNPs) between target (CCRF-CEM cells are actually CCL-119 T-cell) and control cells (Ramos cells are CRL-1596, B-cell), reprinted with permission from [55], Copyright 2006 American Chemical Society.

reported that this method could detect 50 nM to 500 fM of DNA by adjusting silver enhancement time [50]. This method showed 10 times more sensitivity and 10^6 times more specificity over current genomic detection systems [50].

Recently, Herr et al. reported that a novel two nanoparticles assay can be used to extract and detect acute leukemia cells rapidly [55]. They used aptamer modified magnetic and fluorescent nanoparticles simultaneously. First, magnetic nanoparticles extracted the target cells from the sample solution, and subsequently fluorescent nanoparticles enhanced the sensitivity of the detection. The magnetic extraction efficiency for the target cells was well above that for control cells, as shown in Figure 6. To improve the sensitivity even further, fluorescent nanoparticles were used with the magnetic nanoparticles. To compare the fluorescent enhancement capabilities of dye-doped nanoparticles over aptamer conjugated fluorescent dye, individual dye (Rubpy) probes were linked with the aptamer in order to be immobilized on target cells. Equal amounts of magnetic and Rubpy nanoparticles were incubated with target cells and then washed three times by magnetic extraction. The sensitivity of dye-doped nanoparticles was at least 100 times higher than that for the aptamer conjugated fluorescent dye, as shown in Figure 7. The simultaneous use of two different aptamer-conjugated nanoparticles on the same target enhanced the selectivity significantly. Only magnetic extraction separated a good number of target cells from control cells, but due to nonspecific binding, some control cells were also retained in the extracted solution, as shown in Figure 8. Simultaneous incorporation of the fluorescent nanoparticles along with the magnetic extraction enhanced the selectivity even further, which is much desired for practical applications. Very high sensitivity is always required to analyze a real sample due to the low ratio of target cells to other cells.

Recently, Lee et al. have also reported multimodal probing of tumor cells using iron oxide nanoparticles with thermally crosslinked polymer shells [56]. They synthesized triblock polymer (poly(3-(trimethoxysilyl) propyl methacrylate-r-PEG methyl ether methacrylate)), denoted as poly(TMSMA-r-PEGMA), for coating the iron oxide nanoparticles. Figure 9 shows the coating and crosslinking of the polymer on the surface of nanoparticles. The thermally crosslinked superparamagnetic iron oxide nanoparticles were denoted as TCL-SPION. The N-hydrosuccinimide-activated carboxylic acid group provided active sites for the further conjugation of fluorescent dyes (such as near-infrared dyes) for optical imaging and cancer-specific ligands [57]. $Si(OCH_3)_3$ group provided the bonding to iron oxide and the crosslinking of the polymer shells and PEG for biocompatibility [56].

Magnetic resonance imaging (MRI) showed the tumor as a hyperintense area in T_2-weighted images, as shown in Figure 10(a) with a red arrow and a dashed circle before the injection of the Cy5.5 TCL-SPION. At 3.5 hours after the injection, MRI showed a decrease in signal, implying the accumulation of the SPION within tumor region. This decrease in signal was sufficient for a radiologist to detect the tumor with high confidence. *In vivo* fluorescence images of the same mouse at similar time points were also taken, as shown in Figure 10(b). The pseudo-color-adjusted optical images showed a relatively intense fluorescence signal exclusively in the tumor area (red arrow in Figure 10(b)) at 3.5 h postinjection time. This result perfectly agreed with the MR imaging results. The *in vivo* T_2 MR and near-infrared (NIR) fluorescent imaging of tumor-bearing mice after the intravenous injection of the Cy5.5 conjugated multimodal probes revealed that the probes were accumulated at the tumor site due to enhanced permeation and retention effect. This dual imaging technique ensured the detection of tumors with good confidence.

In order to investigate further, *ex vivo* NIR fluorescent images of several organs and tumors were taken. They indicated that the highest fluorescence intensity was observed in the tumor region. When the free Cy5.5 dye without nanoparticles was intravenously injected into a tumor-bearing mouse as a control experiment, only a faint fluorescence signal was observed in the tumor [56].

2.3. Nanopores. A nanopore is a nanoscale channel or hole in a freestanding membrane. Solid-state nanopores were originally inspired from reports of biological transmembrane proteins being used as nanopores and nanoscale detectors. For example, the alpha-hemolysin (αHL) channel was used to detect small molecules of single stranded nucleic acids in the seminal paper by Kasianowicz et al. [58]. More recently, Clarke et al. have shown that a modified αHL nanopore (as shown in Figure 11) can be used to distinguish individual DNA mononucleotides [59]. As a mononucleotide base passes through the pore, the ionic current is modulated in a more or less base-specific manner. Pulse depth is a measure of how strongly the base interacts with the pore and depth of pulse distribution is used to discriminate among different bases. Although a given DNA base (e.g., dAMP) does not yield a uniform pulse depth, the pulse distribution is largely distinguishable between the four DNA bases, as shown in Figure 12(b). There is some degree of overlap between consecutive distributions that can introduce

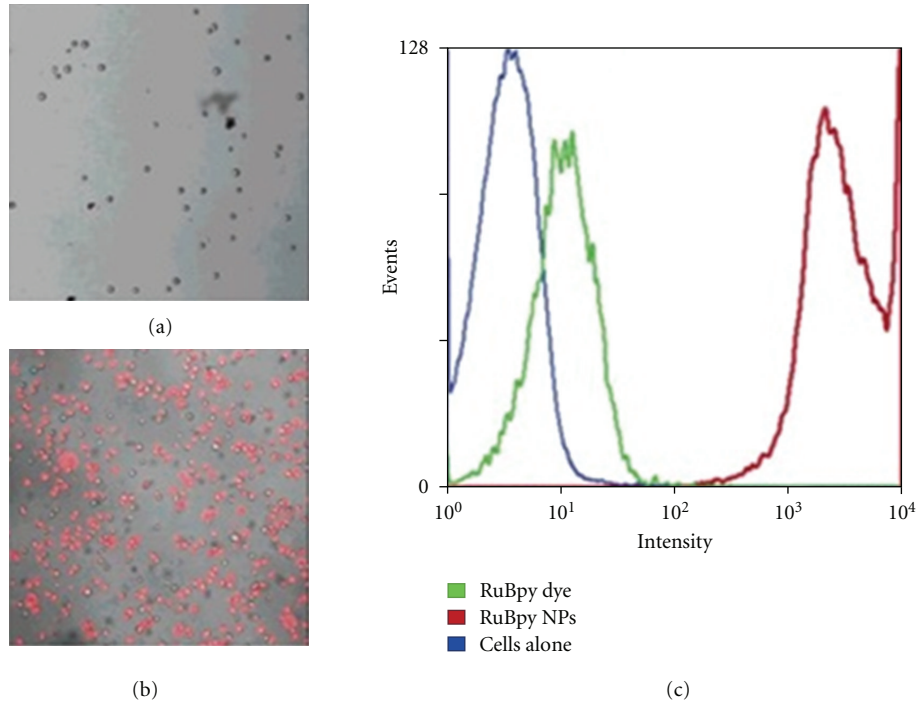

Figure 7: Fluorescence images of extracted cells after 5 min incubation followed by three magnetic washes with (a) Rubpy dye-aptamer conjugates (40 μM) and (b) Rubpy nanoparticle-aptamer conjugates (0.5 nM). (c) Comparative plots between dye-labeled cells and NP-labeled cells by flow cytometric analysis, reprinted with permission from [55], Copyright 2006 American Chemical Society.

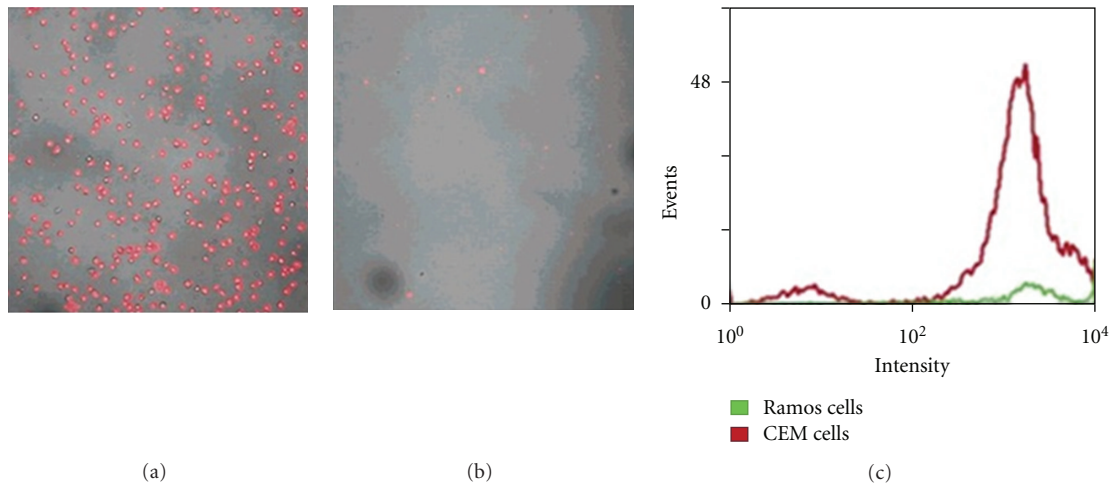

Figure 8: (a) Sample from target cells, (b) sample extracted from control cells, and (c) flow cytometric comparison between target and control signal after 5 min incubation followed by three magnetic washes with magnetic and fluorescent nanoparticles, reprinted with permission from [55], Copyright 2006 American Chemical Society.

detection errors. A mutant αHL and a covalently attached adapter protein ($am_6amPDP_1\beta CD$), however, can enhance the base discrimination, thereby reducing errors (see the current pulses and histograms in Figure 12) [59].

Figure 13 shows that each of four DNA mononucleotides had characteristic pore current distribution. The four distributions were centered around four distinct current levels; that is, signals from each base were separable. This method was capable of discriminating between the four DNA nucleotides (dAMP, dTMP, dCMP, and dGMP) with over 99% confidence under optimal operating condition [59].

Such reports show the potential of nanopores toward the ultimate goal of direct sequencing of single molecules of DNA. A reliable, low-cost DNA sequencing can have a profound effect on genome research. DNA sequence information can provide useful information about an individual's genetic makeup that might put someone at increased risk for certain diseases like cancer. Apart from medical applications,

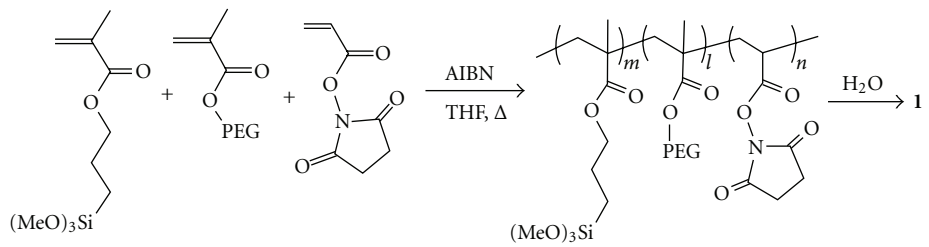

Poly(TMSMA-γ-PEGMA-γ-NAS)
($m : l : n = 0.85 : 1 : 0.71$)

(a)

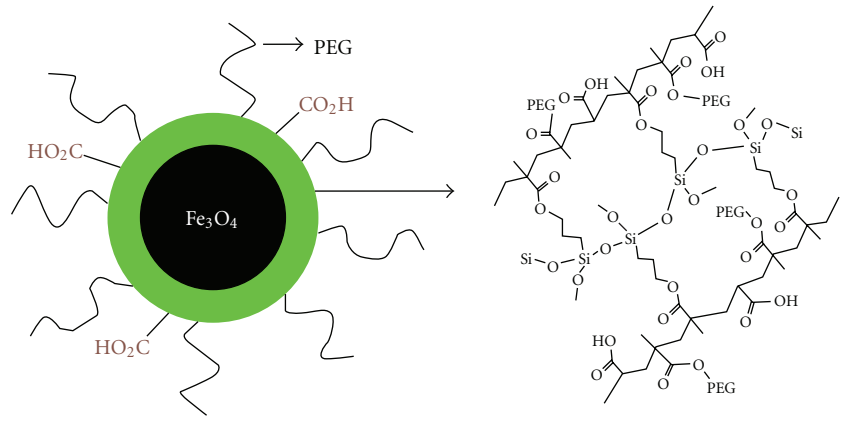

Carboxyl TCL-SPION

Crosslinked polymeric shell

(b)

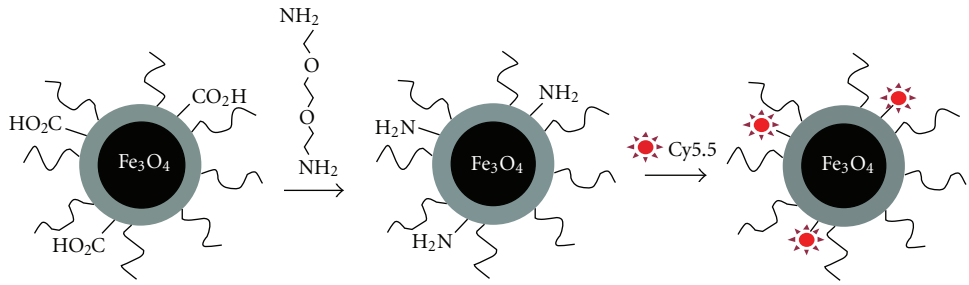

Carboxyl TCL-SPION Amino TCL-SPION Cy5.5 TCL-SPION

	Carboxyl TCL-SPION	Amino TCL-SPION	Cy5.5 TCL-SPION
Size (DLS)	25.6 ± 2.7 nm	32.6 ± 3.7 nm	31.9 ± 4.6 nm
Zeta potential	−30.5 mV	−1.34 mV	−25.13 mV

(c)

Figure 9: (a) Method of synthesis of poly (TMSMA-r-PEGMA-r-NAS); (b) schematic representation of carboxyl TCL-SPION crosslinking between polymer layers after heat treatment; and (c) amino and Cy5.5 TCL-SPION with different size and zeta potential, reprinted with permission from [56]. Copyright 2007, American Chemical Society.

there are many other application areas, such as agriculture, security, defense, and evolutionary biology, where genomic information is useful [33].

Solid-state nanopores (also called artificial nanopores) are made using many types of membrane materials (silicon, SiO_2, and Si_3N_4) and by opening the orifice using a number of different approaches. A recent review on solid-state nanopores used for nucleic acid detection succinctly describes various approaches [25]. The paper delineates both the advances and the many remaining hurdles. Although focused on nucleic acid analysis, this paper lays out advancements that have been achieved through last 15 years and

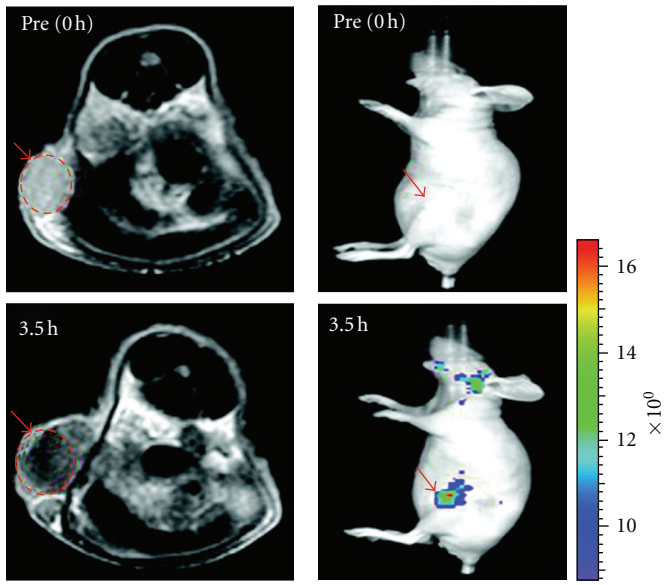

Figure 10: (a) T_2-weighted MR images (TR/TE of 4200 ms/102 ms) taken after 0 and 3.5 h of injection of 14.7 mg Fe/kg in PBS of Cy5.5 TCL-SPION at the level of tumor (320 mm^3). The allograft tumor region is dashed with red circle. (b) Fluorescence images of the same mouse under same condition. An exposure time of 1 s and a Cy5.5 filter channel were used. The scale on the right indicates the relative fluorescence intensity, reprinted with permission from [56]. Copyright 2007, American Chemical Society.

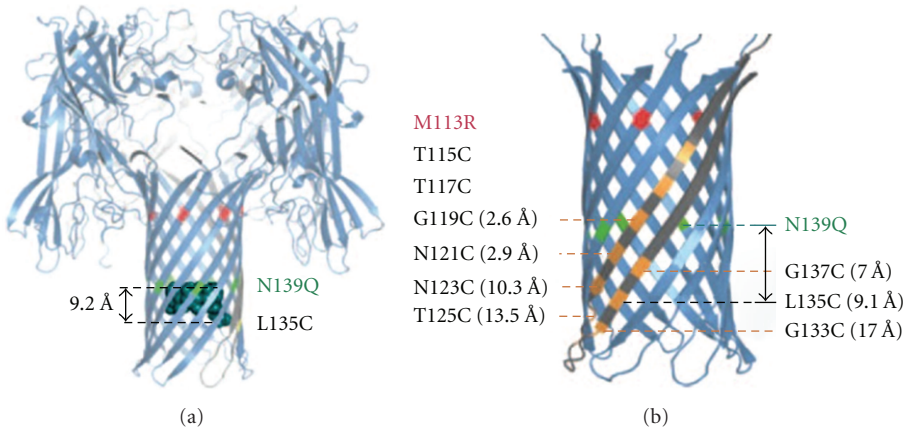

Figure 11: (a) Structure of the WT $(M113R/N139Q)_6$ $(M113R/N139Q/L135C)_1$ mutant (cartoon view) showing the covalent attachment of cyclodextrin at position 135 (space filling model), the glutamines at residue 139, and the vertical distance between the secondary hydroxyls and the disulphide bond of the cyclodextrin. (b) β barrel structure showing the location of arginines (at position 113) and the cysteines in the mutants. Single letter standard amino acid code was used to describe the mutants, reprinted by permission from Nature Publishing Group: Nature Nanotechnology [59], copyright 2009.

clearly defines challenges that have impeded applications of nanopore sensors in general. Most important challenges include needs for high spatial resolution, algorithms for complex analysis and severe lack of chemical engineering approaches for nanopores towards selective and sensitive detection. A recent book has also appeared that describes the whole range of nanopore fabrication approaches as well as targets of detection [24].

One such fabrication approach used polydimethylsiloxane (PDMS), a common polymer used to create microfluidic channels and microscale devices (Figure 14) [60]. The nanoscale device was created by sealing a PDMS mold containing two reservoirs connected by a pore with a glass cover slip. It was then filled with an ionic solution. The potential across the pore was measured at constant applied current by using a four-point technique. When DNA molecules were passed through the pore, they partially blocked the flow of ions, giving a downward spike in the current profile, as shown in Figure 15. Each downward peak corresponded to a single DNA molecule passing through the pore. No current dip was observed in the absence of DNA. By tweaking the pore sizes to slightly larger dimensions, it is

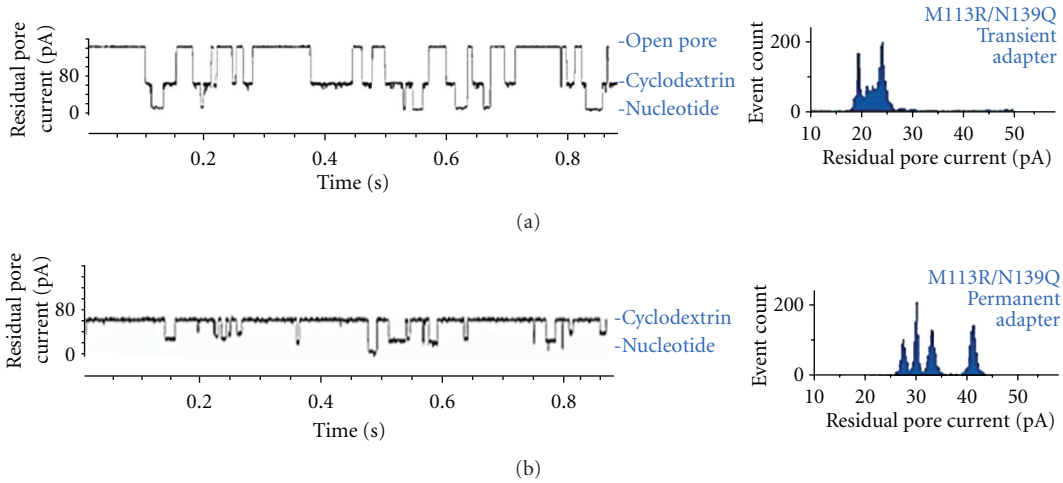

Figure 12: Comparison of recording from single channel of permanent and transient adapters. (a) The WT-$(M113R/N139Q)_7$ αHL pore illustrating transient adapter binding (40 mM am7βCD) and nucleotide detection. Nucleotide binding events histogram for residual current. (b) Corresponding data for the WT-$(M113R/N139Q)_6$ $(M113R/N139Q/L135C)_1$ mutant with a covalently bonded $am_6amPDP_1\beta CD$, allowing continuous nucleotide detection and enhanced nucleotide discrimination. The traces were recorded under the parameter set up of 800 mM KCl, 25 mM Tris HCl, pH 7.5, at +160 mV in the presence of 10 μM dGMP, 10 μM dTMP, 10 μM dAMP, and 10 μM dCMP, reprinted by permission from Nature Publishing Group: Nature Nanotechnology [59], copyright 2009.

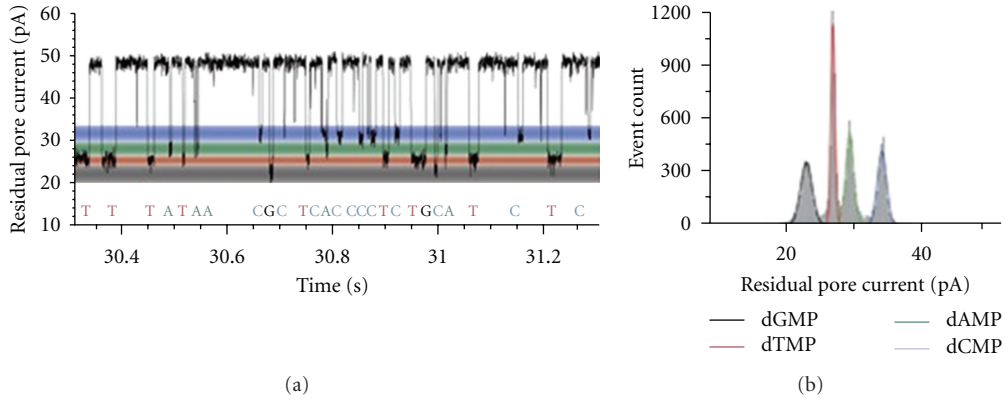

Figure 13: Distribution of nucleotide event with the permanent adapter. (a) Single-channel recording from the WT-$(M113R/N139Q)_6(M113R/N139Q/L135C)_1$-$am_6amPDP_1\beta CD$ pore showing dGMP, dTMP, dAMP, and dCMP discrimination with a Gaussian fits. (b) Corresponding residual current histogram of nucleotide binding events, including Gaussian fits. Data acquired under the condition of 400 mM KCl, 25 mM Tris HCl, pH 7.5, at +180 mV in the presence of 10 μM dGMP, 10 μM dTMP, 10 μM dAMP, and 10 μM dCMP, reprinted by permission from Nature Publishing Group: Nature Nanotechnology [59], copyright 2009.

also possible to detect viruses or proteins [61, 62]. Covalently attaching probe molecules to the pore wall have allowed such devices to detect specific target species [61].

Specific target detection is also possible by measuring the change in size of a chemically functionalized colloid upon binding target molecules [60]. Saleh and Sohn reported an antibody-antigen-binding detection system based on a PDMS nanopore [22]. They functionalized the surface of colloidal particles with biocompatible material. When the particle passed through the pore, it left a signature of current blockade depending on its size. A particle with larger diameter took more time to pass and created higher dips in the current profile [22]. Antibody was specifically bound to the colloid surface, increasing its diameter. The increased size of the particle resulted in higher resistance in the current flow. Size-dependent discrimination was based on the translocation time and the current dip. Therefore, this device had the potential to detect an antigen corresponding to the antibody attached to the colloid surface by comparing the difference in the current profile [22]. This technique was used to detect presence of *Streptococcus* group A. The sensitivity of detection was compared to that of a standard latex agglutination assay, and it was found that the former method was an order of magnitude more sensitive than the agglutination assay. It was also four times faster [22].

Nanopore-based detection systems require small sample volumes and can count and distinguish among a variety of different biological molecules in a complex mixture using

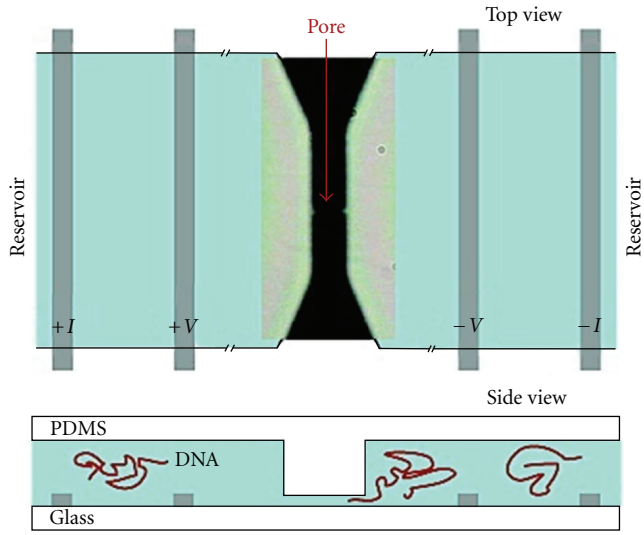

Figure 14: Top and side views of the nanopore device consisting of two 5 μm deep reservoirs connected by a lateral pore of 3 μm length and 200 nm diameter, reprinted with permission from [60], Copyright 2003 American Chemical Society.

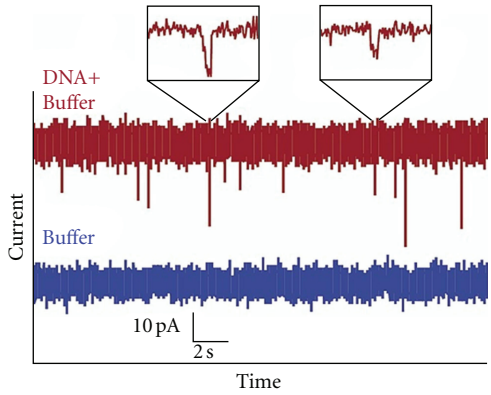

Figure 15: Current versus time plot of buffer solution (lower trace) and buffer with λ-phage DNA molecules (upper trace) upon application of 0.4 V across the pore. Every dip in current profile represents a DNA molecule passing through the pore. The pulse widths are typically 2–10 ms in duration and are well resolved, as shown in the insets. The variations in peak height are attributed to the different conformation of each molecule, reprinted with permission from [60], Copyright 2003 American Chemical Society.

simple electronic measurements. The cost-effectiveness, simplicity, speed, and versatility of nanopore assays is poised to expedite the development of molecular diagnostics [23].

2.4. Carbon Nanotubes. A carbon nanotube (CNT) is an allotrope of graphite. Carbon atoms are hexagonally connected in a CNT lattice. CNTs can be visualized as single or multiple graphite sheets rolled to form a cylindrical structure. Depending on the number of sheets, there are two types of CNTs: single wall carbon nanotubes (SWCNTs) and multiwall carbon nanotubes (MWCNTs). These are also classified as armchair, zigzag, and chiral based on the orientation of atoms on the sheet with respect to the axes. Depending on how carbon atoms are oriented on the CNT surface, their electronic, chemical, and mechanical properties can change. Armchair CNTs are preferred to be used as electrodes in biosensors [63].

Li et al. developed a DNA microarray system which contained sensing pads constructed from assembled MWCNTs that were built into a matrix within a silicon nitride template, as shown in Figure 16 [64]. The open ends of nanotubes acted as nanoelectrodes. By combining such a nanoelectrode platform with Ru(bpy)32+-mediated guanine oxidation, target oligonucleotides at few attomoles could be detected with this method. The sensitivity could be further improved by increasing the number of nanotubes in one cluster. It was reported that the system was capable of providing fast, cheap, and simple molecular diagnostic solutions for medical and field uses [64]. In a recent study, Wang et al. showed that CNTs coated with alkaline phosphatase (ALP) enzymes as labels amplified the signal-to-noise ratio [65]. The CNTs were modified with oligonucleotides that were complementary to half of the target DNA sequence.

Magnetic microparticles modified with oligonucleotides complementary to the other half of the target DNA sequence were used. As shown in Figure 17, while there was target DNA present in the sample, a sandwich of magnetic nanoparticles-target-CNT was formed which was magnetically separated from the assay [65]. R-naphthyl phosphate was added to the extract in order to detect the ALP-modified CNTs. The presence of ALP in the mixture changed the R-naphthyl phosphate into R-naphthol, which was detected by the CNT-modified electrodes using a method called chronopotentiometric stripping. Reportedly, this method could detect very low concentrations of DNA (54 attomoles) [65].

2.5. Nanowires. A nanowire is a rodlike structure with diameter on the order of a few nanometers and an unconstrained length. Self-limiting oxidation has been used to fabricate silicon nanowires [66, 67]. To create an array, a silicon-on-insulator (SOI) wafer was patterned and etched as shown

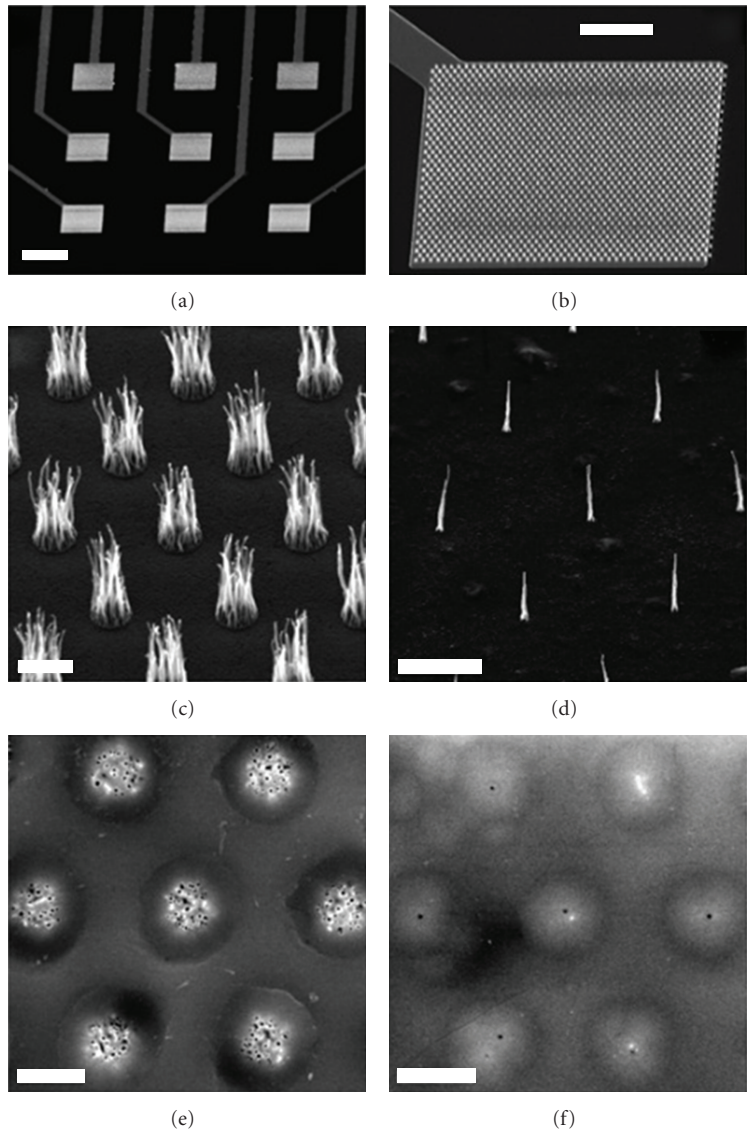

Figure 16: SEM micrographs of (a) 3×3 Ni electrode array, (b) array of MWCNT bundles on an electrode pad, (c) and (d) array of MWCNTs on Ni spots patterned by UV-lithography and e-beam lithography, respectively, (e) and (f) the surface of polished MWCNT array electrodes grown on 2 μm and 200 nm spots, respectively. 45° perspective view was used for (a–d) and (e-f) were top views. The scale bars for (a), (b), (c), (d), (e), and (f) are 200, 50, 2, 5, 2, and 2 μm, respectively, reprinted with permission from [64], Copyright 2003 American Chemical Society.

in Figure 18 [15]. The fin structures were further oxidized and stripped of the oxide layer to realize the nanowires. A metallization step was followed to establish contact to the nanowires. Isolation of electrodes from each other and from the substrate was provided by using an oxide and buried oxide layer, respectively. An encapsulation was used to isolate all electrical contacts from the aqueous solution [15].

Gao et al. reported a method of DNA detection using silicon nanowires. Peptide nucleic acid (PNA) probes were immobilized onto the nanowire surfaces by silane chemistry, as shown in Figure 19 [15]. The PNA probes were allowed to hybridize with target DNA. Hybridization, in turn, induced a change in the resistance of the nanowires. The use of PNA over DNA gave twofold advantages: bonding strength of PNA-DNA is higher than that of a DNA-DNA pair due to the absence of negatively charged phosphate groups in PNA, and resistance change due to nonspecific binding of DNA was less in the case of PNA probes [68, 69]. The calibration curve was plotted as shown in Figure 20 [15]. The relationship between relative change in resistance and the logarithm of DNA concentration was approximately linear over a range of 1 nM to 0.1 fM. The relative error associated with the detection method described was less than 25% [70]. Hahm and Lieber also reported similar sensitivity of silicon nanowire sensor to detect DNA, albeit with high background noise [71].

Signal strength must be enhanced to make these silicon nanowire sensors as practical devices. Nanowire-based

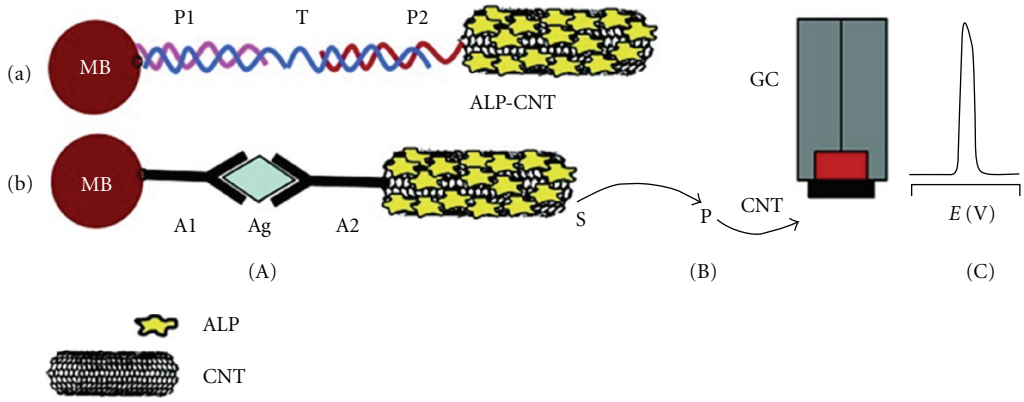

Figure 17: (A) Schematic illustration of capture of the alkaline-phosphate-(ALP-) coated CNT tags to the streptavidin-modified magnetic beads by (a) a sandwich DNA hybridization (b) Ab-Ag-Ab interaction. (B) Enzymatic reaction. (C) Electrochemical detection of the product produced from enzymatic reaction at the CNT-modified glassy carbon electrode, reprinted with permission from [65], Copyright 2001 American Chemical Society. MB: magnetic beads; P1: DNA probe 1, T: DNA target, P2: DNA probe 2, AB1: first antibody, Ag: antigen, Ab2: secondary antibody, S and P: substrate and product, respectively; GC: glassy carbon electrode, and CNT: carbon nanotube layer.

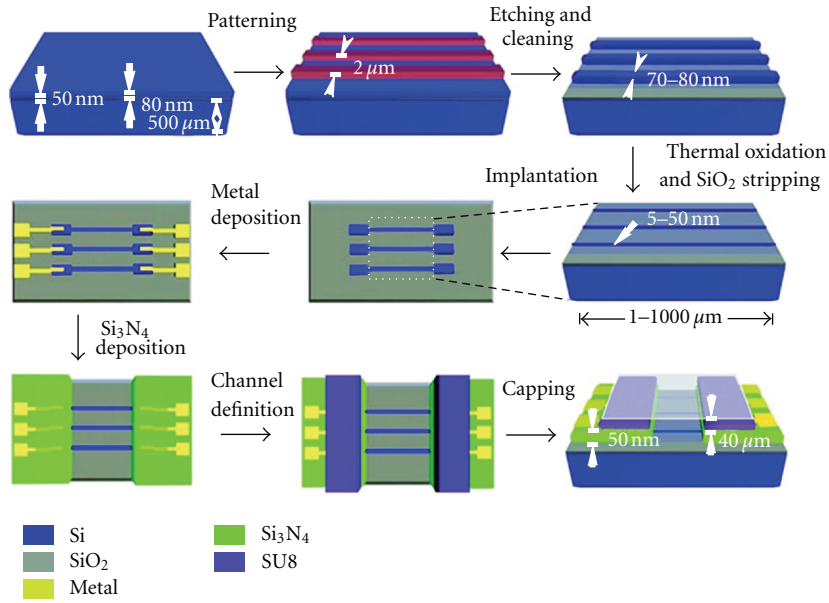

Figure 18: Schematic illustration of the fabrication process of Silicon nanowire arrays with fluidic channels, reprinted with permission from [15], Copyright 2007 American Chemical Society.

detection methods can be used for multiplexed bioanalysis [72–74]. Semiconductor nanowire-based FETs can be used to provide ultrasensitive label-free detection of biomolecular interactions [75]. Electrical conductance is the parameter to be monitored to detect binding events occurring on the nanowire surface.

A PNA-modified nanowire was used as FET to selectively detect specific DNA molecules [71]. The high sensitivity was attributed to the small diameter of the nanowires. The binding of the target molecules on the surface of nanowires caused accumulation or depletion of charges, which led to a change in the channel conductance. This technique also has been used to detect proteins, ions, and viruses with high sensitivity [75–77].

The same group developed silicon nanowire FETs with control nanowires in the same assay that gave a way to eliminate false-positive results [78]. Reportedly, a femtomolar concentration of protein markers was repeatedly detected with the device. The nanowire array provided highly selective and sensitive multiplexed detection of prostate-specific antigen (PSA), PSA-*a*1-antichymotrypsin, carcinoembryonic antigen, and mucin-1, all biomarkers for cancer [78]. Using an undiluted serum sample, they achieved a detection limit of 0.9 pg/mL. Telomerase activity was also monitored by using nucleic acid functionalized real-time nanowire assays. The capability of multiplexed real-time monitoring of protein biomarker and telomerase activity with high sensitivity and selectivity is very important

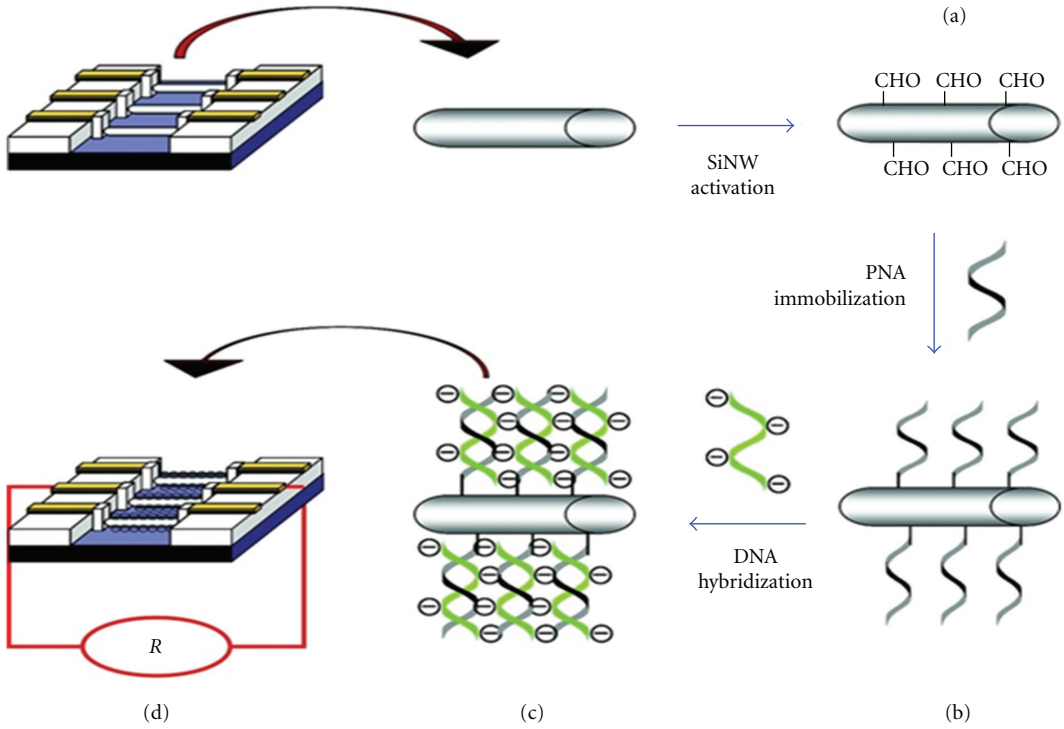

Figure 19: Operating principle of the silicon nanowire array biosensor for DNA detection, reprinted with permission from [15]. Copyright 2007 American Chemical Society.

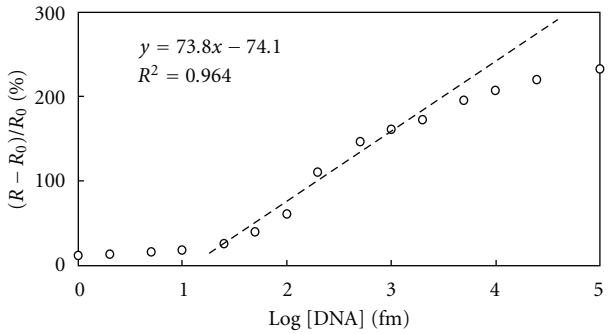

Figure 20: Calibration profile for target oligonucleotides detection with a linear fit (Operating condition 60 min hybridization at 50°C), reprinted with permission from [15]. Copyright 2007 American Chemical Society.

clinically to diagnose cancer early and then to monitor disease progression [78].

Barcoded metallic nanowires, synthesized by template electrodeposition of multiple metal segments, were reported to have the potential to be used as suspension array to detect protein and nucleic acid simultaneously [73, 74]. Multiplexed detection of biothreat simulants, including protein, spore, and viral targets were reported with high sensitivities using metallic nanowires array [79]. The detection limit of this assay could be scaled by reducing the total number of barcoded nanowires. Sha et al. reported that their barcoded nanowires system was capable of performing 30 different assays simultaneously to determine the genotypes of single-nucleotide polymorphisms (SNPs) [80].

Very recently, Chua et al. developed a silicon nanowire array-based assay that was capable of providing ultrasensitive, label-free electrical detection of a cardiac biomarker in real time. This assay proved itself to be effective to detect ultralow concentrations of a target protein in a biological analyte solution, even in the presence of a high total protein concentration. The high specificity, selectivity, and swift response time from this method serves the need of medical diagnostic systems for point-of-care applications to provide early and accurate indication of cardiac cellular necrosis [81].

Nanowire-based detection systems provide a flexible multiplexing scheme to detect biomolecules simultaneously. They offer ultrasensitive electrical detection without any labeling, which is the prime requirement to develop a portable, low-power microchip-based device that can process multiplexed data from many individual sensors. The use of such devices would not be limited to clinical environments; they could be used outside the clinical environment where availability of medical facilities is limited.

2.6. Nanosheets. A nanosheet is a single- or multilayer two-dimensional array of atoms or molecules. Graphene is a flat monolayer of carbon atoms arranged in a two-dimensional honeycomb crystal structure [82]. It is a basic building block for graphitic materials of all other dimensionalities. High thermal conductivity (~5000 W/m K) [83], high specific surface area, high electron mobility (250,000 cm^2/Vs) [84], easily achievable biocompatibility, and exceptional thermal

stability make it a material of choice for fabricating electrochemical immunosensors [82, 85–88].

Wang et al. reported that graphene oxide nanosheets (GO-nS) could be used to probe *in vivo* cellular interactions [89]. These nanosheets could be used as DNA cargo and sensing platforms. The unique interaction between GO-nS and DNA molecules was exploited to produce an aptamer/GO-nS complex, which was used as a real-time biosensing platform in living cells. In the experiments, they used a fluorescently tagged ATP-binding aptamer (FAM-aptamer) to elucidate the use of GO-nS as (i) a sensing platform with high fluorescence quenching efficiency for realizing real-time *in vivo* target monitoring, (ii) DNA transporter into living cells, and (iii) efficient protection of oligonucleotides from enzymatic cleavage [89]. ATP was targeted because it is of medical interest. ATP is a central molecule involved in cellular metabolism and bioenergetics. Figure 21 shows the schematic illustration of the experiment. FAM-Aptamer was loaded onto GO-nS. The FAM florescence was quenched by the GO-nS in the GO-nS bound state. In the presence of ATP, ATP-aptamer complexes formed and released from the GO-nS. The released ATP-aptamer complexes were detectable by the FAM fluorescence [89].

In order to investigate the sensing performance of the aptamer/GO-nS complex, *in vitro* ATP detection was carried out first. Initially, fluorescent quenching was observed due to the fluorescent resonance energy transfer (FRET) between FAM and GO-nS. When ATP was present in the solution, it bound to the aptamer, thus releasing the FAM from the GO-nS surface. The released FAM showed the fluorescence activity. Figure 22 shows the fluorescence intensity upon the presence of different amounts of ATP in the solution. It indicates that aptamer-FAM/GO-nS complex had high sensitivity and a wide detection range, from 10 μM to 2.5 mM, for *in vitro* ATP sensing [89]. The specificity of this complex was also good. Only ATP showed an obvious fluorescence recovery up to 85.7%, whereas none of cytidine triphosphate (CTP), guanosine triphosphate (GTP), or thymidine triphosphate (TTP) showed any substantial fluorescence recovery. The good selectivity and sensitivity of the aptamer/GO-nS nanocomplex predicted its potential use for intracellular ATP monitoring in living cells [89].

For *in vivo* analysis, mice epithelial cells (JB6 Cl 41-5a) were chosen. It was seen that only the aptamer-FAM/GO-nS had a significantly higher uptake rate than random DNA/GO-nS or GO-nS alone or aptamer-FAM alone. The GO-nS not only helped to transport the DNA into the cell but also protected it from the enzymatic cleavage.

Figure 23 shows a comparative picture of cellular ATP probing done by aptamer-FAM/GO-nS (g–l) and random DNA/GO-nS (a–f). As time elapsed, the amount of fluorescent signal increased in the case of aptamer-FAM/GO-nS, which showed that the ATP-aptamer duplex was formed; hence, fluorescence was recovered. But for random DNA/GO-nS, no significant increase of fluorescence was observed, which confirmed the hypothesis that GO-nS helped to deliver the aptamer inside the cell and released the aptamer for target detection [89].

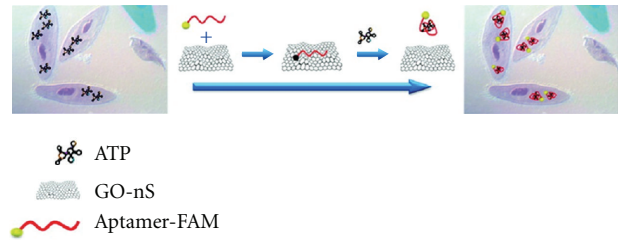

Figure 21: Schematic representation of in situ molecular probing inside living cells using aptamer/GO-nS nanocomplex, reprinted with permission from [89]. Copyright 2010, American Chemical Society.

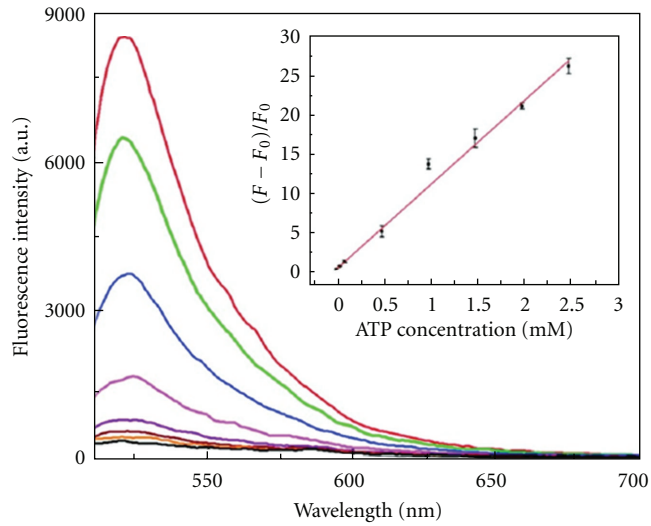

Figure 22: Fluorescence emission spectra of ATP aptamer-FAM quenched (100 nM) with 3 μg/mL GO-nS (black bottom line) and fluorescence recovery by addition of ATP with a concentration range from 10 μM to 2.5 mM (from bottom to top). Inset: linear fit between relative fluorescence intensity and ATP concentration. Given that F_0 and F are the fluorescence intensity without and with the presence of ATP, respectively, reprinted with permission from [89]. Copyright 2010, American Chemical Society.

3. Major Challenges with the Use of Nanostructures

Over the last decade or so, many synthesized nanostructures with at least one dimension in the 1–100 nm range have been created and used to exhibit fascinating physicochemical properties [90, 91]. In addition to their small sizes, these nanostructures have large surface-to-volume ratios and very high reactivities compared to their bulk counterparts. Their very small size allows them to cross many boundaries with ease (e.g., across cell membranes). They can efficiently bind to biological molecules and species such as DNA, RNA, PNA, proteins, and viruses. Owing to the novel properties of nanoscale structures, they have been examined for their potential to be incorporated into various devices, such as sensors, immunoassays, transistors, drug and gene delivery carriers, virus inhibitors, and DNA and protein immobilizers [16, 21, 22, 41, 44, 53, 59, 65, 81, 92–94].

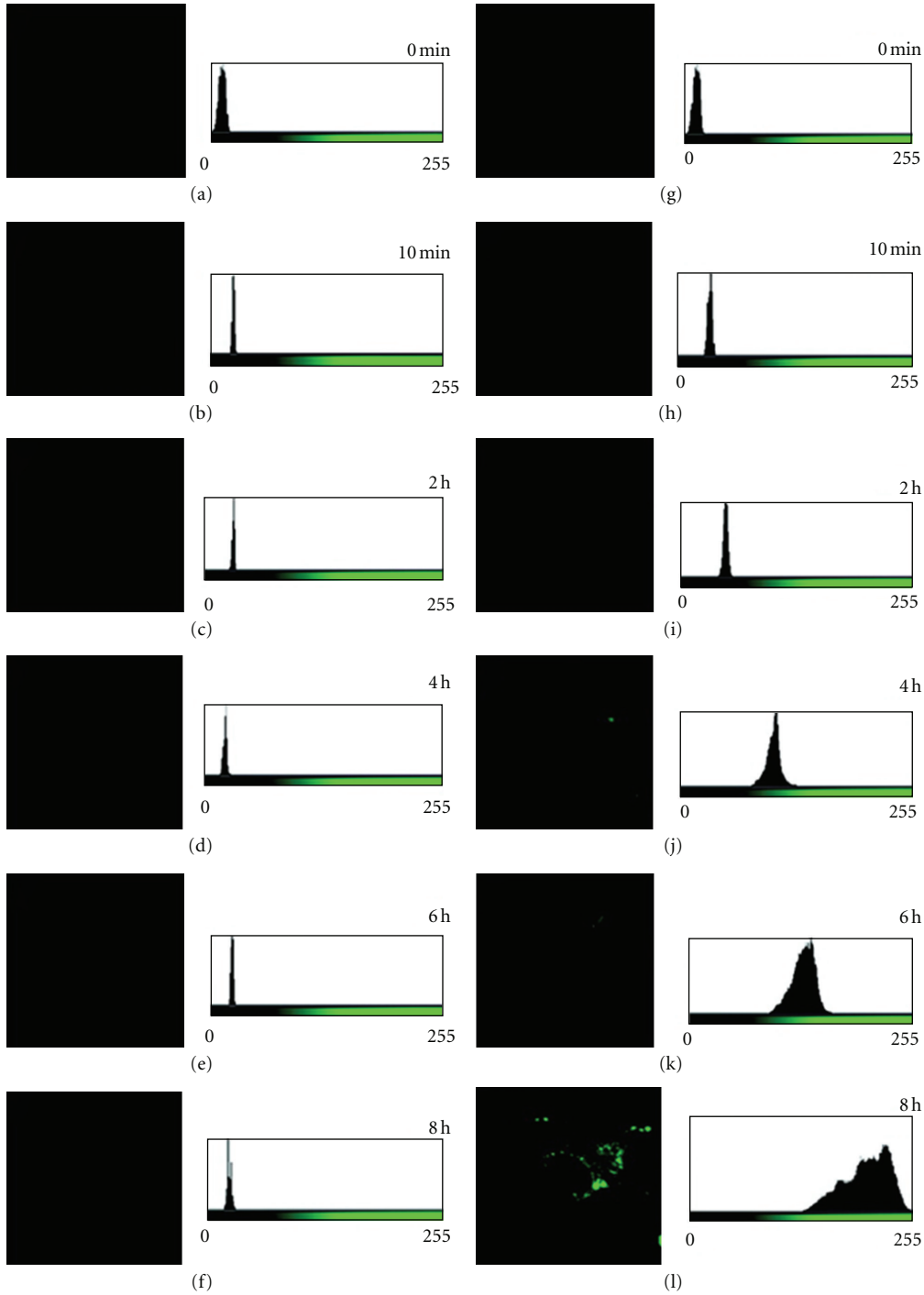

Figure 23: Real-time monitoring of JB6 cells cultured with random DNA-FAM/GO-nS (a–f) and aptamer-FAM/GO-nS (g–l) for 8 h at 37°C. Images were captured every 2 h using a wide-field microscopy every 2 h. Colored bar indicates the fluorescent intensity, reprinted with permission from [89]. Copyright 2010, American Chemical Society.

Although nanodevices have indeed demonstrated great potential, enthusiasm is tempered by the fact that reproducing devices with such dimensions is still a challenge. In addition, short- and long-term toxicological effects of nanoparticles and nanostructures in biological systems are largely unknown. Nanostructures have been reported to produce pulmonary inflammation [95]. They can also reach other organs by passing through the lung epithelium and can reach interstitial tissues [95, 96]. These effects have been shown to be more prevalent in species such as dogs and primates than in rodents [97].

Studies have shown carbon nanotubes to be cytotoxic. They can induce granulomas in the lungs of laboratory animals [98]. *In vitro* studies have demonstrated that

single-wall nanotubes can generate reactive oxygen species in human keratinocytes and human bronchial epithelial cells, indicating that oxidative stress is one of the predominant mechanisms of their acute toxicity [99, 100]. Oxidative stress was identified as the participating mechanism of Ag nanoparticles toxicity in an *in vitro* study with BRL-3A liver cells, supporting the previous notion [101]. Nanoparticles made of metals and metallic oxides such as copper, cobalt, titanium, and silicon oxide have also been shown to have inflammatory and toxic effects on cells [98].

Another *in vitro* study showed that metal nanoparticles disrupted proliferation, damaged cell membranes, and initiated apoptosis in C18-4 and germ-line stem cells [102]. After intraperitoneal administration, fullerenes have been shown to distribute throughout the embryo and yolk sac of mice 18 hours after injection, and they crossed the placental barrier [103]. Rhodamine-labeled silica-coated magnetic nanoparticles passed the blood-testis barrier and aggregated in the seminiferous epithelium where spermatogenesis takes place. After penetration into seminiferous epithelium, the nanoparticles got incorporated into the developing germ cells and eventually became part of mature sperms [104].

Asharani et al. showed that multiwalled CNTs damaged DNA in mouse embryonic stem (ES) cells [105]. In another study it was shown that multiwalled CNTs could accumulate and induce apoptosis in mouse ES cells and activated the tumor suppressor protein p53 within two hours of exposure [106]. The above studies indicate that nanostructures could potentially impact human health by producing oxidative stress, altering DNA, or producing phenotypic damage to the cells.

A necessary step, therefore, is accurately determining nanostructures' properties of interest and understanding their interactions with relevant biological systems. Detailed characterization of such a wide variety of novel structures and their modified versions is required to assess the toxicity or any other threat they may possess. Various synthesis techniques of nanostructures produce a wide variety of structures with different physical characteristics such as size, morphology, surface chemistry, and biological coatings. In a biological context, we need to understand the impacts of these variations in order to improve the existing methods in terms of quality, control, and safety issues. Further studies are required to develop more precise fabrication techniques and to determine the appropriate modifications that will resolve the safety issues.

4. Conclusion

In this review article, we have discussed fabrication techniques of different nanostructures. We have also discussed the applications of these structures in the fields of medical diagnostics. The promise of increased sensitivity and speed with reduced cost and labor makes nanostructure-based assays an appealing alternative to current diagnostic techniques. The potential uses of nanostructures in medical diagnostics are numerous, although some important challenges to implementation exist. Aside from the technical difficulties of nanostructure fabrication, there are serious concerns about nanostructure toxicity and that toxicity may vary depending on the physical characteristics of each new particle type. Further research is required to evaluate and solve these issues. If the issues can be overcome, the high sensitivity, specificity, reduced cost, portability, and reusability of nanostructures will make nanostructures important medical diagnostics tools.

References

[1] X. Huang, I. H. El-Sayed, W. Qian, and M. A. El-Sayed, "Cancer cell imaging and photothermal therapy in the near-infrared region by using gold nanorods," *Journal of the American Chemical Society*, vol. 128, no. 6, pp. 2115–2120, 2006.

[2] P. K. Jain and M. A. El-Sayed, "Universal scaling of plasmon coupling in metal nanostructures: extension from particle pairs to nanoshells," *Nano Letters*, vol. 7, no. 9, pp. 2854–2858, 2007.

[3] P. K. Jain, X. Huang, I. H. El-Sayed, and M. A. El-Sayed, "Noble metals on the nanoscale: optical and photothermal properties and some applications in imaging, sensing, biology, and medicine," *Accounts of Chemical Research*, vol. 41, no. 12, pp. 1578–1586, 2008.

[4] L. Zhang and T. J. Webster, "Nanotechnology and nanomaterials: promises for improved tissue regeneration," *Nano Today*, vol. 4, no. 1, pp. 66–80, 2009.

[5] H. Shen, X. Hu, J. Bei, and S. Wang, "The immobilization of basic fibroblast growth factor on plasma-treated poly(lactide-co-glycolide)," *Biomaterials*, vol. 29, no. 15, pp. 2388–2399, 2008.

[6] J. Carpenter, D. Khang, and T. J. Webster, "Nanometer polymer surface features: the influence on surface energy, protein adsorption and endothelial cell adhesion," *Nanotechnology*, vol. 19, no. 50, Article ID 505103, 2008.

[7] S. Moon, W. Song, N. Kim et al., "Current-carrying capacity of double-wall carbon nanotubes," *Nanotechnology*, vol. 18, no. 23, Article ID 235201, 2007.

[8] J. G. Park, S. Li, R. Liang, X. Fan, C. Zhang, and B. Wang, "The high current-carrying capacity of various carbon nanotube-based buckypapers," *Nanotechnology*, vol. 19, no. 18, Article ID 185710, 2008.

[9] F. Patolsky, B. P. Timko, G. Zheng, and C. M. Lieber, "Nanowire-based nanoelectronic devices in the life sciences," *MRS Bulletin-Materials Research Society*, vol. 32, no. 2, pp. 142–149, 2007.

[10] K. Kerman, M. Saito, E. Tamiya, S. Yamamura, and Y. Takamura, "Nanomaterial-based electrochemical biosensors for medical applications," *TrAC—Trends in Analytical Chemistry*, vol. 27, no. 7, pp. 585–592, 2008.

[11] S. E. Brunker, K. B. Cederquist, and C. D. Keating, "Metallic barcodes for multiplexed bioassays," *Nanomedicine*, vol. 2, no. 5, pp. 695–710, 2007.

[12] L. G. Carrascosa, M. Moreno, M. Alvarez, and L. M. Lechuga, "Nanomechanical biosensors: a new sensing tool," *TrAC—Trends in Analytical Chemistry*, vol. 25, no. 3, pp. 196–206, 2006.

[13] Y. J. Seo, J. Lim, E. H. Lee et al., "Base pair opening kinetics study of the aegPNA: DNA hydrid duplex containing a site-specific GNA-like chiral PNA monomer," *Nucleic Acids Research*, vol. 39, no. 16, pp. 7329–7335, 2011.

[14] J. B. Raoof, R. Ojani, S. M. Golabi, E. Hamidi-Asl, and M. S. Hejazi, "Preparation of an electrochemical PNA biosensor

for detection of target DNA sequence and single nucleotide mutation on p53 tumor suppressor gene corresponding oligonucleotide," *Sensors and Actuators, B: Chemical*, vol. 157, no. 1, pp. 195–201, 2011.

[15] Z. Gao, A. Agarwal, A. D. Trigg et al., "Silicon nanowire arrays for label-free detection of DNA," *Analytical Chemistry*, vol. 79, no. 9, pp. 3291–3297, 2007.

[16] J. Fritz, M. K. Baller, H. P. Lang et al., "Translating biomolecular recognition into nanomechanics," *Science*, vol. 288, no. 5464, pp. 316–318, 2000.

[17] M. Ferrari, "Cancer nanotechnology: opportunities and challenges," *Nature Reviews Cancer*, vol. 5, no. 3, pp. 161–171, 2005.

[18] S. Wolf and R. N. Tauber, *Silicon Processing for the VLSI Era: Process Technology*, vol. 1, Lattice Press, Sunset Beach, Calif, USA, 1986.

[19] D. Xia, D. Li, Z. Ku, Y. Luo, and S. R. J. Brueck, "Top-down approaches to the formation of silica nanoparticle patterns," *Langmuir*, vol. 23, no. 10, pp. 5377–5385, 2007.

[20] D. Li, J. T. McCann, Y. Xia, and M. Marquez, "Electrospinning: a simple and versatile technique for producing ceramic nanofibers and nanotubes," *Journal of the American Ceramic Society*, vol. 89, no. 6, pp. 1861–1869, 2006.

[21] E. Stern, J. F. Klemic, D. A. Routenberg et al., "Label-free immunodetection with CMOS-compatible semiconducting nanowires," *Nature*, vol. 445, no. 7127, pp. 519–522, 2007.

[22] O. A. Saleh and L. L. Sohn, "Direct detection of antibody-antigen binding using an on-chip artificial pore," *Proceedings of the National Academy of Sciences of the United States of America*, vol. 100, no. 3, pp. 820–824, 2003.

[23] K. K. Jain, "Nanodiagnostics: application of nanotechnology in molecular diagnostics," *Expert Review of Molecular Diagnostics*, vol. 3, no. 2, pp. 153–161, 2003.

[24] S. M. Iqbal and R. Bashir, Eds., *Nanopores: Sensing and Fundamental Biological Interactions*, Springer, New York, NY, USA, 2011.

[25] B. M. Venkatesan and R. Bashir, "Nanopore sensors for nucleic acid analysis," *Nature Nanotechnology*, vol. 6, no. 10, pp. 615–624, 2011.

[26] V. Balzani, "Nanoscience and nanotechnology: a personal view of a chemist," *Small*, vol. 1, no. 3, pp. 278–283, 2005.

[27] N. A. Ochekpe, P. O. Olorunfemi, and N. C. Ngwuluka, "Nanotechnology and drug delivery part 1: background and applications," *Tropical Journal of Pharmaceutical Research*, vol. 8, no. 3, pp. 265–274, 2009.

[28] S. Rauf, A. Glidle, and J. M. Cooper, "Production of quantum dot barcodes using biological self-assembly," *Advanced Materials*, vol. 21, no. 40, pp. 4020–4024, 2009.

[29] S. A. E. Valentin, A. Filoramo, A. Ribayrol et al., "Self-assembly fabrication of high performance carbon nanotubes based FETs," *Materials Research Society Symposium Proceedings*, vol. 772, pp. 201–207, 2003.

[30] T. Liu, C. Burger, and B. Chu, "Nanofabrication in polymer matrices," *Progress in Polymer Science*, vol. 28, no. 1, pp. 5–26, 2003.

[31] P. Hyman, R. Valluzzi, and E. Goldberg, "Design of protein struts for self-assembling nanoconstructs," *Proceedings of the National Academy of Sciences of the United States of America*, vol. 99, no. 13, pp. 8488–8493, 2002.

[32] D. Shu, W. D. Moll, Z. Deng, C. Mao, and P. Guo, "Bottom-up assembly of RNA arrays and superstructures as potential parts in nanotechnology," *Nano Letters*, vol. 4, no. 9, pp. 1717–1723, 2004.

[33] D. D. Majumder, R. Banerjee, C. Ulrichs, I. Mewis, and A. Goswami, "Nano-materials: science of bottom-up and top-down," *The Institution of Electronics and Telecommunication Engineers*, vol. 24, no. 1, pp. 9–25, 2007.

[34] M. Shimomura and T. Sawadaishi, "Bottom-up strategy of materials fabrication: a new trend in nanotechnology of soft materials," *Current Opinion in Colloid and Interface Science*, vol. 6, no. 1, pp. 11–16, 2001.

[35] K. K. Jain, "Applications of nanobiotechnology in clinical diagnostics," *Clinical Chemistry*, vol. 53, no. 11, pp. 2002–2009, 2007.

[36] K. K. Jain, "Nanotechnology in clinical laboratory diagnostics," *Clinica Chimica Acta*, vol. 358, no. 1-2, pp. 37–54, 2005.

[37] D. C. Miller, A. Thapa, K. M. Haberstroh, and T. J. Webster, "Endothelial and vascular smooth muscle cell function on poly(lactic-co-glycolic acid) with nano-structured surface features," *Biomaterials*, vol. 25, no. 1, pp. 53–61, 2004.

[38] Y. Wan, M. A. I. Mahmood, N. Li et al., "Nanotextured substrates with immobilized aptamers for cancer cell isolation and cytology," *Cancer*, vol. 118, no. 4, pp. 1145–1154, 2012.

[39] P. Kim, D. H. Kim, B. Kim et al., "Fabrication of nanostructures of polyethylene glycol for applications to protein adsorption and cell adhesion," *Nanotechnology*, vol. 16, no. 10, pp. 2420–2426, 2005.

[40] K. P. S. Dancil, D. P. Greiner, and M. J. Sailor, "A porous silicon optical biosensor: detection of reversible binding of IgG to a protein A-modified surface," *Journal of the American Chemical Society*, vol. 121, no. 34, pp. 7925–7930, 1999.

[41] L. M. Demers, D. S. Ginger, S. J. Park, Z. Li, S. W. Chung, and C. A. Mirkin, "Direct patterning of modified oligonucleotides on metals and insulators by dip-pen nanolithography," *Science*, vol. 296, no. 5574, pp. 1836–1838, 2002.

[42] A. Bruckbauer, L. Ying, A. M. Rothery et al., "Writing with DNA and protein using a nanopipet for controlled delivery," *Journal of the American Chemical Society*, vol. 124, no. 30, pp. 8810–8811, 2002.

[43] K.-B. Lee, E.-Y. Kim, C. A. Mirkin, and S. M. Wolinsky, "The use of nanoarrays for highly sensitive and selective detection of human immunodeficiency virus type 1 in plasma," *Nano Letters*, vol. 4, no. 10, pp. 1869–1872, 2004.

[44] H. K. Kang, J. Seo, D. D. Carlo, Y. K. Choi, and L. P. Lee, "Planar nanogap capacitor arrays on quartz for optical and dielectric bioassays," in *Proceedings of the Micro Total Analsysis Systems*, pp. 697–700, Squaw Valley, Calif, USA, 2003.

[45] C. Buzea, I. I. Pacheco, and K. Robbie, "Nanomaterials and nanoparticles: sources and toxicity," *Biointerphases*, vol. 2, no. 4, 55 pages, 2007.

[46] E. Boisselier and D. Astruc, "Gold nanoparticles in nanomedicine: preparations, imaging, diagnostics, therapies and toxicity," *Chemical Society Reviews*, vol. 38, no. 6, pp. 1759–1782, 2009.

[47] Y. Fu, P. Li, T. Wang et al., "Novel polymeric bionanocomposites with catalytic Pt nanoparticles label immobilized for high performance amperometric immunoassay," *Biosensors and Bioelectronics*, vol. 25, no. 7, pp. 1699–1704, 2010.

[48] A. D. McFarland, C. L. Haynes, C. A. Mirkin, R. P. van Duyne, and H. A. Godwin, "Color my nanoworld," *Journal of Chemical Education*, vol. 81, no. 4, p. 544, 2004.

[49] P. Baptista, E. Pereira, P. Eaton et al., "Gold nanoparticles for the development of clinical diagnosis methods," *Analytical and Bioanalytical Chemistry*, vol. 391, no. 3, pp. 943–950, 2008.

[50] S. J. Park, T. A. Taton, and C. A. Mirkin, "Array-based electrical detection of DNA with nanoparticle probes," *Science*, vol. 295, no. 5559, pp. 1503–1506, 2002.

[51] H. M. E. Azzazy, M. M. H. Mansour, and S. C. Kazmierczak, "Nanodiagnostics: a new frontier for clinical laboratory medicine," *Clinical Chemistry*, vol. 52, no. 7, pp. 1238–1246, 2006.

[52] P. K. Jain, K. S. Lee, I. H. El-Sayed, and M. A. El-Sayed, "Calculated absorption and scattering properties of gold nanoparticles of different size, shape, and composition: applications in biological imaging and biomedicine," *Journal of Physical Chemistry B*, vol. 110, no. 14, pp. 7238–7248, 2006.

[53] L. M. Liz-Marzán, "Tailoring surface plasmons through the morphology and assembly of metal nanoparticles," *Langmuir*, vol. 22, no. 1, pp. 32–41, 2006.

[54] C. Y. Zhang, H. C. Yeh, M. T. Kuroki, and T. H. Wang, "Single-quantum-dot-based DNA nanosensor," *Nature Materials*, vol. 4, no. 11, pp. 826–831, 2005.

[55] J. K. Herr, J. E. Smith, C. D. Medley, D. Shangguan, and W. Tan, "Aptamer-conjugated nanoparticles for selective collection and detection of cancer cells," *Analytical Chemistry*, vol. 78, no. 9, pp. 2918–2924, 2006.

[56] H. Lee, K. Y. Mi, S. Park et al., "Thermally cross-linked superparamagnetic iron oxide nanoparticles: synthesis and application as a dual imaging probe for cancer in vivo," *Journal of the American Chemical Society*, vol. 129, no. 42, pp. 12739–12745, 2007.

[57] A. Moore, Z. Medarova, A. Potthast, and G. Dai, "In vivo targeting of underglycosylated MUC-1 tumor antigen using a multimodal imaging probe," *Cancer Research*, vol. 64, no. 5, pp. 1821–1827, 2004.

[58] J. J. Kasianowicz, E. Brandin, D. Branton, and D. W. Deamer, "Characterization of individual polynucleotide molecules using a membrane channel," *Proceedings of the National Academy of Sciences of the United States of America*, vol. 93, no. 24, pp. 13770–13773, 1996.

[59] J. Clarke, H. C. Wu, L. Jayasinghe, A. Patel, S. Reid, and H. Bayley, "Continuous base identification for single-molecule nanopore DNA sequencing," *Nature Nanotechnology*, vol. 4, no. 4, pp. 265–270, 2009.

[60] O. A. Saleh and L. L. Sohn, "An artificial nanopore for molecular sensing," *Nano Letters*, vol. 3, no. 1, pp. 37–38, 2003.

[61] J. D. Uram, K. Ke, A. J. Hunt, and M. Mayer, "Submicrometer pore-based characterization and quantification of antibody-virus interactions," *Small*, vol. 2, no. 8-9, pp. 967–972, 2006.

[62] A. Han, M. Creus, G. Schürmann et al., "Label-free detection of single protein molecules and protein-protein interactions using synthetic nanopores," *Analytical Chemistry*, vol. 80, no. 12, pp. 4651–4658, 2008.

[63] R. H. Baughman, A. A. Zakhidov, and W. A. de Heer, "Carbon nanotubes—the route toward applications," *Science*, vol. 297, no. 5582, pp. 787–792, 2002.

[64] J. Li, H. T. Ng, A. Cassell et al., "Carbon nanotube nanoelectrode array for ultrasensitive DNA detection," *Nano Letters*, vol. 3, no. 5, pp. 597–602, 2003.

[65] J. Wang, G. Liu, and M. R. Jan, "Ultrasensitive electrical biosensing of proteins and DNA: carbon-nanotube derived amplification of the recognition and transduction events," *Journal of the American Chemical Society*, vol. 126, no. 10, pp. 3010–3011, 2004.

[66] H. I. Liu, D. K. Biegelsen, F. A. Ponce, N. M. Johnson, and R. F. W. Pease, "Self-limiting oxidation for fabricating sub-5 nm silicon nanowires," *Applied Physics Letters*, vol. 64, no. 11, pp. 1383–1385, 1994.

[67] N. Singh, A. Agarwal, L. K. Bera et al., "High-performance fully depleted silicon nanowire (diameter 5 nm) gate-all-around CMOS devices," *IEEE Electron Device Letters*, vol. 27, no. 5, pp. 383–386, 2006.

[68] T. Ratilainen, A. Holmén, E. Tuite, P. E. Nielsen, and B. Nordén, "Thermodynamics of sequence-specifc binding of PNA to DNA," *Biochemistry*, vol. 39, no. 26, pp. 7781–7791, 2000.

[69] M. Egholm, O. Buchardt, L. Christensen et al., "PNA hybridizes to complementary oligonucleotides obeying the Watson-Crick hydrogen-bonding rules," *Nature*, vol. 365, no. 6446, pp. 566–568, 1993.

[70] J. J. Schmidt and C. D. Montemagno, "Using machines in cells," *Drug Discovery Today*, vol. 7, no. 9, pp. 500–503, 2002.

[71] J. I. Hahm and C. M. Lieber, "Direct ultrasensitive electrical detection of DNA and DNA sequence variations using nanowire nanosensors," *Nano Letters*, vol. 4, no. 1, pp. 51–54, 2004.

[72] B. He, T. J. Morrow, and C. D. Keating, "Nanowire sensors for multiplexed detection of biomolecules," *Current Opinion in Chemical Biology*, vol. 12, no. 5, pp. 522–528, 2008.

[73] S. R. Nicewarner-Pena, R. G. Freeman, B. D. Reiss et al., "Submicrometer metallic barcodes," *Science*, vol. 294, no. 5540, pp. 137–141, 2001.

[74] C. D. Keating and M. J. Natan, "Striped metal nanowires as building blocks and optical tags," *Advanced Materials*, vol. 15, no. 5, pp. 451–454, 2003.

[75] F. Patolsky, G. Zheng, and C. M. Lieber, "Nanowire-based biosensors," *Analytical Chemistry*, vol. 78, no. 13, pp. 4260–4269, 2006.

[76] Y. Cui, Q. Wei, H. Park, and C. M. Lieber, "Nanowire nanosensors for highly sensitive and selective detection of biological and chemical species," *Science*, vol. 293, no. 5533, pp. 1289–1292, 2001.

[77] F. Patolsky, G. Zheng, and C. M. Lieber, "Fabrication of silicon nanowire devices for ultrasensitive, label-free, real-time detection of biological and chemical species," *Nature Protocols*, vol. 1, no. 4, pp. 1711–1724, 2006.

[78] G. Zheng, F. Patolsky, Y. Cui, W. U. Wang, and C. M. Lieber, "Multiplexed electrical detection of cancer markers with nanowire sensor arrays," *Nature Biotechnology*, vol. 23, no. 10, pp. 1294–1301, 2005.

[79] B. H. T. Jeffrey, F. Y. S. Chuang, M. C. Kao et al., "Metallic striped nanowires as multiplexed immunoassay platforms for pathogen detection," *Angewandte Chemie—International Edition*, vol. 45, no. 41, pp. 6900–6904, 2006.

[80] M. Y. Sha, I. D. Walton, S. M. Norton et al., "Multiplexed SNP genotyping using nanobarcode particle technology," *Analytical and Bioanalytical Chemistry*, vol. 384, no. 3, pp. 658–666, 2006.

[81] J. H. Chua, R. E. Chee, A. Agarwal, S. M. Wong, and G. J. Zhang, "Label-free electrical detection of cardiac biomarker with complementary metal-oxide semiconductor-compatible silicon nanowire sensor arrays," *Analytical Chemistry*, vol. 81, no. 15, pp. 6266–6271, 2009.

[82] A. K. Geim and K. S. Novoselov, "The rise of graphene," *Nature Materials*, vol. 6, no. 3, pp. 183–191, 2007.

[83] A. A. Balandin, S. Ghosh, W. Bao et al., "Superior thermal conductivity of single-layer graphene," *Nano Letters*, vol. 8, no. 3, pp. 902–907, 2008.

[84] K. I. Bolotin, K. J. Sikes, Z. Jiang et al., "Ultrahigh electron mobility in suspended graphene," *Solid State Communications*, vol. 146, no. 9-10, pp. 351–355, 2008.

[85] Y. Song, K. Qu, C. Zhao, J. Ren, and X. Qu, "Graphene oxide: intrinsic peroxidase catalytic activity and its application to glucose detection," *Advanced Materials*, vol. 22, no. 19, pp. 2206–2210, 2010.

[86] B. Su, J. Tang, J. Huang et al., "Graphene and nanogold-functionalized immunosensing interface with enhanced sensitivity for one-step electrochemical immunoassay of α-fetoprotein in human serum," *Electroanalysis*, vol. 22, no. 22, pp. 2720–2728, 2010.

[87] Z. Zhong, W. Wu, D. Wang et al., "Nanogold-enwrapped graphene nanocomposites as trace labels for sensitivity enhancement of electrochemical immunosensors in clinical immunoassays: carcinoembryonic antigen as a model," *Biosensors and Bioelectronics*, vol. 25, no. 10, pp. 2379–2383, 2010.

[88] D. Du, Z. Zou, Y. Shin et al., "Sensitive immunosensor for cancer biomarker based on dual signal amplification strategy of graphene sheets and multienzyme functionalized carbon nanospheres," *Analytical Chemistry*, vol. 82, no. 7, pp. 2989–2995, 2010.

[89] Y. Wang, Z. Li, D. Hu, C. T. Lin, J. Li, and Y. Lin, "Aptamer/graphene oxide nanocomplex for in situ molecular probing in living cells," *Journal of the American Chemical Society*, vol. 132, no. 27, pp. 9274–9276, 2010.

[90] V. L. Colvin, "The potential environmental impact of engineered nanomaterials," *Nature Biotechnology*, vol. 21, no. 10, pp. 1166–1170, 2003.

[91] E. Oberdörster, "Manufactured nanomaterials (fullerenes, C60) induce oxidative stress in the brain of juvenile largemouth bass," *Environmental Health Perspectives*, vol. 112, no. 10, pp. 1058–1062, 2004.

[92] J. M. Nam, C. S. Thaxton, and C. A. Mirkin, "Nanoparticle-based bio-bar codes for the ultrasensitive detection of proteins," *Science*, vol. 301, no. 5641, pp. 1884–1886, 2003.

[93] T. A. Taton, C. A. Mirkin, and R. L. Letsinger, "Scanometric DNA array detection with nanoparticle probes," *Science*, vol. 289, no. 5485, pp. 1757–1760, 2000.

[94] T. L. Lasseter, W. Cai, and R. J. Hamers, "Frequency-dependent electrical detection of protein binding events," *Analyst*, vol. 129, no. 1, pp. 3–8, 2004.

[95] A. Nemmar, A. Delaunois, B. Nemery et al., "Inflammatory effect of intratracheal instillation of ultrafine particles in the rabbit: role of C-fiber and mast cells," *Toxicology and Applied Pharmacology*, vol. 160, no. 3, pp. 250–261, 1999.

[96] S. Utsunomiya, K. A. Jensen, G. J. Keeler, and R. C. Ewing, "Direct identification of trace metals in fine and ultrafine particles in the Detroit urban atmosphere," *Environmental Science and Technology*, vol. 38, no. 8, pp. 2289–2297, 2004.

[97] K. J. Nikula, K. J. Avila, W. C. Griffith, and J. L. Mauderly, "Sites of particle retention and lung tissue responses to chronically inhaled diesel exhaust and coal dust in rats and cynomolgus monkeys," *Environmental health perspectives*, vol. 105, supplement 5, pp. 1231–1234, 1997.

[98] K. A. D. Guzmán, M. R. Taylor, and J. F. Banfield, "Environmental risks of nanotechnology: national nanotechnology initiative funding, 2000–2004," *Environmental Science and Technology*, vol. 40, no. 5, pp. 1401–1407, 2006.

[99] C. Grabinski, S. Hussain, K. Lafdi, L. Braydich-Stolle, and J. Schlager, "Effect of particle dimension on biocompatibility of carbon nanomaterials," *Carbon*, vol. 45, no. 14, pp. 2828–2835, 2007.

[100] A. A. Shvedova, E. Kisin, A. Murray et al., "Exposure of human bronchial cells to carbon nanotubes caused oxidative stress and cytotoxicity," 2004.

[101] S. M. Hussain, K. L. Hess, J. M. Gearhart, K. T. Geiss, and J. J. Schlager, "In vitro toxicity of nanoparticles in BRL 3A rat liver cells," *Toxicology in Vitro*, vol. 19, no. 7, pp. 975–983, 2005.

[102] L. Braydich-Stolle, S. Hussain, J. J. Schlager, and M. C. Hofmann, "In vitro cytotoxicity of nanoparticles in mammalian germline stem cells," *Toxicological Sciences*, vol. 88, no. 2, pp. 412–419, 2005.

[103] T. Tsuchiya, I. Oguri, Y. N. Yamakoshi, and N. Miyata, "Novel harmful effects of [60] fullerene on mouse embryos in vitro and in vivo," *FEBS Letters*, vol. 393, no. 1, pp. 139–145, 1996.

[104] J. S. Kim, T. J. Yoon, K. N. Yu et al., "Toxicity and tissue distribution of magnetic nanoparticles in mice," *Toxicological Sciences*, vol. 89, no. 1, pp. 338–347, 2006.

[105] P. V. Asharani, N. G. B. Serina, M. H. Nurmawati, Y. L. Wu, Z. Gong, and S. Valiyaveettil, "Impact of multi-walled carbon nanotubes on aquatic species," *Journal of Nanoscience and Nanotechnology*, vol. 8, no. 7, pp. 3603–3609, 2008.

[106] S. M. Hussain, L. K. Braydich-Stolle, A. M. Schrand et al., "Toxicity evaluation for safe use of nanomaterials: recent achievements and technical challenges," *Advanced Materials*, vol. 21, no. 16, pp. 1549–1559, 2009.